



FACULTAD DE CIENCIAS

Theoretical and computational study of a mathematical model for cancer tumor growth, including chemotherapy

Estudio teórico y computacional de un modelo
matemático para el crecimiento de tumores
cancerígenos, incluyendo quimioterapia.

TRABAJO DE FIN DE GRADO
PARA ACCEDER AL
GRADO EN MATEMÁTICAS

Author: Isabel Lasheras Bujanda

Director: Luis Alberto Fernández Fernández

July 2023

Agradecimientos

Con este trabajo pongo fin a mi carrera de Matemáticas, y no puedo menos que agradecer a todos aquellos que lo habéis hecho posible.

En primer lugar, a Luis Alberto, mi director. Por tu esfuerzo, tu confianza y tu tiempo. Tu compromiso y dedicación me han transmitido, desde el principio, las ganas de esforzarme por sacar adelante este trabajo. Gracias también por haberme escuchado, orientado y aconsejado en todo momento, y por esmerarte tanto en aclarar mis dudas y en enseñarme. Tu cercanía y apoyo me han hecho disfrutar al máximo de cada etapa de la realización de este trabajo.

A mis padres, mi ejemplo a seguir. De quienes he aprendido a disfrutar del trayecto que, cerca o lejos de casa, me lleva a conseguir mis objetivos. Por nunca dejar que me rindiera y por hacerme ver que todo esfuerzo tiene su recompensa. A mi hermano Javier, a mi abuelo Ignacio, al enano y a toda mi familia, en especial a los que me cuidáis desde ahí arriba. Gracias por confiar en mí, saber que estáis orgullosos de mí ha sido y será siempre mi motivación.

Gracias, cómo no, a mis amigos, especialmente a mi cuadrilla y mis amigas de Nazar, por alegraros de mis logros como si fueran los vuestros y por apoyarme en todo momento.

Gracias Cecilia por tu ayuda, y gracias a todos los profesores que habéis participado en mi formación por haberme hecho constatar mi amor por las matemáticas.

Gracias, resumiendo, a quienes habéis estado a mi lado a lo largo de esta etapa de mi vida, que ha hecho de mí quien soy hoy.

Abstract

Cancer tumor growth can be studied using mathematical models. In this work, we will focus on the model proposed by P. Hahnfeldt et al. for the growth of some cancer tumors and on its variant with the logistic model. These models consider not only the tumor volume, but also the physiological process in which new blood vessels are produced, angiogenesis, due to its big impact on the tumor evolution. They are composed by a system of two nonlinear ODE (Ordinary Differential Equations), where new terms can be included aiming to model the effect of the treatment of chemotherapy applied (cytotoxic, antiangiogenic, or combined).

In this report we include the theoretical study of the system's asymptotic behavior when the concentration of the administered drug is constant and when it varies along time. We also include several computational experiments, carried out with MATLAB, that aim to distinguish between the two cases that can arise when a drug is administered: the tumor evolution is the expected, or it is counter intuitive. The experiments will also show the evolution of the concentration of the drug in the body, and they intend to identify the most suitable combinations of chemotherapy treatments.

Keywords: Chemotherapy, anti angiogenic drugs, cytotoxic drugs, Hahnfeldt et al. model, Norton-Simon hypothesis, computational experiments.

Resumen

El crecimiento de algunos tumores cancerígenos puede ser estudiado haciendo uso de modelos matemáticos. En este trabajo, nos centraremos en el modelo propuesto por P. Hahnfeldt et al. y en su variante usando el modelo logístico. Dichos modelos contemplan también el proceso fisiológico a través del cual se forman nuevos vasos sanguíneos, conocido como angiogénesis, que influye notablemente en la evolución del tumor. Constan de un sistema de dos EDO (Ecuaciones Diferenciales Ordinarias) no lineales al que, para modelizar el efecto de la aplicación de un tratamiento de quimioterapia (citotóxico, antiangiogénico o combinado), se le pueden añadir nuevos términos.

En esta memoria se recoge el estudio teórico del comportamiento asintótico de este sistema para el caso en que la concentración del fármaco se mantiene constante así como para el caso en que cambia con el tiempo. También se realizarán, con la ayuda de MATLAB, varios experimentos computacionales que servirán para distinguir las distintas situaciones que pueden darse al administrar tratamiento. Estas situaciones se clasificarán en función de si el resultado es el esperado o si es contraintuitivo. Los experimentos permitirán estudiar también la evolución de la concentración de fármaco en el cuerpo y tratarán de identificar la combinación más adecuada de diferentes tipos de quimioterapia.

Palabras clave: Quimioterapia, fármaco antiangiogénico, fármaco citotóxico, modelo de Hahnfeldt et al., hipótesis de Norton-Simon, experimentos computacionales.

Contents

1	Introduction	1
1.1	Cancer	2
1.2	Structure of the work	2
2	Tumor growth models	4
2.1	Gompertz and logistic models	4
2.2	Hahnfeldt model	5
2.3	Hahnfeldt model variant with logistic	13
3	PK/PD	15
3.1	Pharmacokinetics	15
3.2	Pharmacodynamics	17
3.2.1	Cytotoxic effect	17
3.2.2	Antiangiogenic effect	18
3.2.3	Cytotoxic antiangiogenic effect	18
3.3	Keeping concentration near a constant value	25
4	Computational experiments	26
4.1	Parameters	26
4.1.1	Equispaced administration times	27
4.1.2	Temozolomide	28
4.2	Cytotoxic treatment	28
4.2.1	Choice of k_1 and k_2	29
4.2.2	Administration in N doses	30
4.2.3	Initial points	32
4.2.4	Comparing administration ways	36
4.3	Combining different treatments	39
4.3.1	Combining treatments: experiments	40
4.4	MATLAB programs	47
5	Conclusions	49

Chapter 1

Introduction

The origins of medicine can be traced back to prehistory. Since the beginning, discovering treatments able to cure or to palliate the symptoms of different illnesses has been its main purpose. Nevertheless, not only is it crucial to find the medicament to apply, but also the correct administration doses: if the quantity of drug is not enough, it may not have the effect wondered and if, instead, too much is given, it can be toxic for the patient. Aristotle described this perfectly: *in medio virtus*. A similar fact takes place when considering the administration times: numerous studies must be carried out in order to determine the ones that will have the desired results avoiding harmful or lethal consequences.

It is widely known that this kind of decisions are not taken from one day to the next: for instance, pharmacokinetics-pharmacodynamics relations of the drug selected have large effects on the choices made, as well as individual particularities of each body. Therefore, aiming to generalize the conclusions with minimal risks, countless experiments are done. This procedure is what precedes the major milestones in medicine. In these experiments, in order to purchase a relatively good inference, an appropriate sample size is needed. And, when it comes to health, it is important to have a sample large enough to consider as many cases as possible and to reduce the errors of the estimates.

Traditionally, these tests have involved expensive research expenditures: experimental animals are subjected to different conditions in order to provide proofs that a treatment is efficient and safe enough to be applied in humans. Nevertheless, these experiments are not always preceded by as many studies as necessary, which provokes polemical discussions about its ethics and morality. This situation also presents the problem of the results not always being reliable due to the differences between animals and humans. This fact makes more difficult the translation from bench to bedside even if, aiming to avoid it, animals are genetically modified (which implies a bigger cost).

Nonetheless, new techniques have emerged during the past decades, and mathematics have had a big impact on medicine. Mathematical models have given great advances in

biology since they provide the possibility of doing feasible predictions on natural phenomena. Additionally, computational simulations are useful to carry out experiments in a much more efficient way. Although they can not substitute the totality of traditional tests, these simulations can relieve the quantity of lives that are risked in the typical ones, as the results observed can help to discard many experiments before being done on living things.

Moreover, *in silico* experiments are a reliable option when considering unusual illnesses: it is not hard to find a big sample of patients suffering flu, i.e; nevertheless, when the intention is to study a particular type of tumor, it may be complicated to find a sufficient amount of people presenting this disease. Computational experiments permit the replication of peculiar conditions and let multiple trials be done.

1.1 Cancer

The National Cancer Institute (NCI) of the United States defines cancer as “a disease in which some of the body’s cells grow uncontrollably and spread to other parts of the body” (see [17]). It is one of the principal death causes in the world: the International Agency for Research of Cancer registered almost 10 million deaths due to cancer during 2020, being around 19,3 millions the number of new cases diagnosed that year (see [14]).

Computational oncology has contributed to the study of cancer and, although its use remains insufficient in practice, it can help to enhance the anti-cancer treatments. Within others like surgery, immunotherapy or radiotherapy, chemotherapy is one of the most utilized treatments. During it, drugs are administered in order to kill or shrink cancer cells. They can be given in many different ways: the two best known are the Maximum Tolerated Dose (MTD) and the metronomic chemotherapy, where more, but smaller, doses are administered (see the introduction of [8]).

Usually, cytotoxic drugs are applied during the chemotherapy process. This kind of drugs have direct effects on the tumor cells, killing or reducing them. Nevertheless, these are not the only drugs that are used in order to combat the disease. Angiogenesis is a multi-stage process during which new capillary blood vessels are generated. It was found that tumors make use of this process to grow, as they get the nutrients and the oxygen needed for they survival from blood vessels (see [4]). Therefore, there exist anti-angiogenic therapies, whose target is the tumor’s vasculature (the blood vessels that surround the tumor).

1.2 Structure of the work

It is noteworthy the fact that not only the tumor depends on its vasculature, but also the vasculature depends on the tumor, as it spells secretions which promote or obstruct angiogenesis. In particular, mathematical models are of service when studying the evo-

lution of the tumor and its vasculature when a treatment is applied (and when it is not), as well as the pharmacokinetics and pharmacodynamics of the drugs used.

Therefore, in this work we will make use of them. We will start by considering two typical growth models, the one by Gompertz, adapted to this particular case by Hahnfeldt, and the logistic one. Using them to formulate a system of two Ordinary Differential Equations (ODE), in Chapter 2 we will try to study the behavior of both the volume and the vasculature of the tumor according to different parameters. For this chapter we will concentrate on the mathematical study, not on the biological meaning of the parameters.

We will focus on this in Chapter 3, where we will study the effect of administering different drugs (cytotoxic, anti-angiogenic and combined). We will not only centre on the pharmacodynamics (PD, the effect a drug has on a body), but also on the pharmacokinetics (PK), which investigate drug behavior. To delve into the PK/PD relationships, we will distinguish two cases: first, we will consider that the concentration of the drug in the body takes a constant value. This study will be very similar to the one done in Chapter 2. After it, we will consider that the drug's concentration is not constant, being this more realistic according to the pharmacokinetic study.

How administering a drug affects the tumor's volume and vasculature is usually studied with two different models, which adjust the effect of the drug according to its concentration in the body, so we will end this third chapter by proving that keeping this concentration near a constant value will keep the level of effect in a steady state. We will show how could we keep this concentration near the desired constant value if the doses were administered equispaced and in the same quantity (which may not be completely trustworthy in practice, as many external factors affect administration) in Chapter 4. This chapter corresponds to computational experiments, for which we have used MATLAB.

For these experiments, we must give different values to our parameters, which will determine the administration doses and times. Although we will choose many of them according to other studies, some will be taken in order to make the results plausible, even if they should be determined by specialists. Once chosen, we will compare the evolution of the disease depending on whether no treatment is administered or whether a cytotoxic drug is given, in a continuous way or in discrete doses. To do this, we will take different initial situations, which we will also use in the last section of the chapter, where we will consider different treatment combinations mixing both anti-angiogenic and cytotoxic drugs. These initial cases have been chosen with the aim of distinguishing the different situations that can take place.

Chapter 2

Tumor growth models

2.1 Gompertz and logistic models

With the aim of modeling different natural processes throughout history, biology has made use of mathematical resources. This is the case of the Gompertzian model and the logistic one, which are widely known for being employed in growth phenomena studies (see [21]).

The Gompertz's model is commonly used to adjust populations' data with restrictions such as limited resources, or biological limitations. Its curve, presented in 1825 by Benjamin Gompertz, is given by the following ODE:

$$V'(t) = -\lambda_1 V(t) \log \left(\frac{V(t)}{K} \right), \quad (2.1)$$

where $V(t)$ is the population size at a time t , λ_1 is a positive constant and $K > 0$ is the carrying capacity: the maximum population size that can be reached.

As it is said in [2], it is interesting “how mathematical models could serve as potential prognostic tools in the clinic”. Following in their steps, we will make use of these models in order to study tumor evolution, as “tumor growth kinetics follow relatively simple laws that can be expressed as mathematical models”. Since this model is commonly used to model populations, they (and we too) consider that the tumor volume is proportional to the number of cells in the tumor, and we can therefore relate it to the population of cells, considering now that V is the volume of the tumor (see [2]).

Although the Gompertzian model is, because of this, frequently chosen for situations like tumor growth, there are some issues when it comes to considering $\lim_{V \rightarrow 0^+} \frac{V'}{V}$ as it is not bounded:

$$\lim_{V \rightarrow 0^+} \frac{V'}{V} = \lim_{V \rightarrow 0^+} -\lambda_1 \log \left(\frac{V}{K} \right) = +\infty.$$

The logistic model, which is also described in [21], becomes then a good alternative. The ODE describing its curve is

$$V'(t) = \frac{\lambda_1 V(t)}{K} (K - V(t)), \quad (2.2)$$

where, again, $\lambda_1 > 0$ and $K > 0$ is the carrying capacity.

It is used to model population growth, as well as social magnitudes such as message diffusion, although we can also use it for tumor growth, just as the Gompertzian model. Furthermore, as we have just said, this model is a reliable alternative when we want $\lim_{V \rightarrow 0^+} \frac{V'}{V}$ to be bounded, as in this case

$$\lim_{V \rightarrow 0^+} \frac{V'}{V} = \lim_{V \rightarrow 0^+} \frac{\lambda_1}{K} (K - V) = \lambda_1 < +\infty.$$

We will, therefore, use both models to describe the volume of a tumor.

2.2 Hahnfeldt model

Let $V(t)$ be the tumor volume at a time t . We will use the ideas of [10], where it is explained that, although historically K in (2.1) has been considered a fixed value, in this case it would be more suitable to consider it as a dynamic carrying capacity $K(t)$. This is due to the secretions a tumor expels, affecting its vasculature. Although contemplating this vasculature as a carrying capacity it would be reasonable to assume $V < K$, it has been observed that in practice $K < V$ or $K > V$ depending on whether the tumor is regressing or growing, which has more sense when considered in the context of angiogenesis.

The ODE for the Gompertz's model, taking all this into account, would be:

$$V'(t) = -\lambda_1 V(t) \log \left(\frac{V(t)}{K(t)} \right), \quad (2.3)$$

where λ_1 is the growth rate and the change rate $K'(t)$ can be described as follows

$$K'(t) = -\lambda_2 K(t) + bV(t) - dK(t)V^{2/3}(t), \quad (2.4)$$

being $\lambda_2 \geq 0$ the loss rate and $b > 0$ and $d > 0$ the weights of the stimulator and inhibitory effects from the tumor cells (see [10]). (2.4) has been obtained from equation (C4) in [10], taking $e = 0$ because we will consider at first that administered inhibitors are not applied.

As we have mentioned, the secretions of a tumor have an impact on its vasculature. In addition, due to the nutritive function of the tumor's vasculature, how the vasculature

evolves will also affect the tumor's growth. This is, they are interrelated. We can set up an ODE system in order to study the tumor/vasculature dynamics, which can be written as autonomous system:

$$\begin{cases} V' = f_1(V, K) = -\lambda_1 V \log\left(\frac{V}{K}\right), \\ K' = f_2(V, K) = -\lambda_2 K + bV - dKV^{2/3}, \\ V(0) = V_0 > 0, K(0) = K_0 > 0. \end{cases} \quad (2.5)$$

The domain considered for both functions will be $\Omega = \{(V, K) \in \mathbb{R}^2 : V > 0, K > 0\}$, noting that $f_1(V, K)$ is not defined at $(0, 0)$ (see [13]).

Our intention is to determine how the solutions for the system evolve. This is, how do the volume and the vasculature of the tumor behave as time goes on. We will distinguish several cases depending on the sign of λ_1 and on whether $b > \lambda_2$ or not. For a more schematic view, see Table 2.1 at the end of this section.

Case $\boxed{b > \lambda_2}$: (2.5) has a critical point (V_c, K_c) with $V_c = K_c = \left(\frac{b - \lambda_2}{d}\right)^{3/2}$, which is the point satisfying $f_1(V_c, K_c) = f_2(V_c, K_c) = 0$. The system's local stability around this point can be studied using the Taylor's formula.

The partial derivatives are continuous in Ω and they are:

$$\begin{aligned} \frac{\partial f_1}{\partial V}(V, K) &= -\lambda_1 \log\left(\frac{V}{K}\right) - \lambda_1 \Rightarrow \frac{\partial f_1}{\partial V}(V_c, K_c) = -\lambda_1 \\ \frac{\partial f_1}{\partial K}(V, K) &= \lambda_1 \frac{V}{K} \Rightarrow \frac{\partial f_1}{\partial K}(V_c, K_c) = \lambda_1 \\ \frac{\partial f_2}{\partial V}(V, K) &= b - \frac{2}{3}dKV^{-\frac{1}{3}} \Rightarrow \frac{\partial f_2}{\partial V}(V_c, K_c) = b - \frac{2}{3}dV_c^{\frac{2}{3}} \\ \frac{\partial f_2}{\partial K}(V, K) &= -\lambda_2 - dV^{\frac{2}{3}} \Rightarrow \frac{\partial f_2}{\partial K}(V_c, K_c) = -\lambda_2 - dV_c^{\frac{2}{3}}. \end{aligned}$$

Hence, using $V_c = \left(\frac{b - \lambda_2}{d}\right)^{\frac{3}{2}}$

$$\begin{aligned} f_1(V, K) &\approx f_1(V_c, K_c) + \frac{\partial f_1}{\partial V}(V_c, K_c)(V - V_c) + \frac{\partial f_1}{\partial K}(V_c, K_c)(K - K_c) + \dots \\ &= -\lambda_1(V - V_c) + \lambda_1(K - K_c) + \dots \\ f_2(V, K) &\approx f_2(V_c, K_c) + \frac{\partial f_2}{\partial V}(V_c, K_c)(V - V_c) + \frac{\partial f_2}{\partial K}(V_c, K_c)(K - K_c) + \dots \\ &= \left(b - \frac{2}{3}dV_c^{\frac{2}{3}}\right)(V - V_c) + \left(-\lambda_2 - dV_c^{\frac{2}{3}}\right)(K - K_c) + \dots \\ &= \frac{b + 2\lambda_2}{3}(V - V_c) - b(K - K_c) + \dots \end{aligned}$$

Linearizing we approximate (2.5) as

$$\begin{pmatrix} x' \\ y' \end{pmatrix} = \underbrace{\begin{pmatrix} -\lambda_1 & \lambda_1 \\ \frac{b+2\lambda_2}{3} & -b \end{pmatrix}}_A \begin{pmatrix} x \\ y \end{pmatrix} \quad (2.6)$$

where $x = V - V_c$ and $y = K - K_c$.

The general solution for (2.6) is given by

$$\begin{pmatrix} x \\ y \end{pmatrix} = c_1 e^{\gamma_1 t} \bar{v}_1 + c_2 e^{\gamma_2 t} \bar{v}_2$$

being \bar{v}_1 and \bar{v}_2 the eigenvectors associated to γ_1 and γ_2 , the eigenvalues of matrix A in (2.6):

$$\begin{aligned} \gamma_1 &= \frac{-(\lambda_1 + b)}{2} + \sqrt{\frac{2}{3}\lambda_1(\lambda_2 - b) + \frac{1}{4}(\lambda_1 + b)^2}; \\ \gamma_2 &= \frac{-(\lambda_1 + b)}{2} - \sqrt{\frac{2}{3}\lambda_1(\lambda_2 - b) + \frac{1}{4}(\lambda_1 + b)^2}. \end{aligned}$$

Both γ_1 and γ_2 will be real or not depending on the radicand's sign, so we will distinguish cases in order to determinate it:

1. When $\boxed{\lambda_1 > 0}$, as $b > \lambda_2$, the radicand can be written as sum of positive terms (and thus both eigenvalues will be real) and $\lambda_1(\lambda_2 - b) < 0$, which implies $\gamma_1 < 0$, being clear that $\gamma_2 < 0$. Therefore, $\lambda_1 > 0$ leads us to an asymptotically stable case: $\lim_{t \rightarrow +\infty} e^{\gamma_1 t} = 0$ and $\lim_{t \rightarrow +\infty} e^{\gamma_2 t} = 0$; thus, $\lim_{t \rightarrow +\infty} x(t) = 0$ and $\lim_{t \rightarrow +\infty} y(t) = 0$ which means $\lim_{t \rightarrow +\infty} V(t) = V_c$ and $\lim_{t \rightarrow +\infty} K(t) = K_c$.

This is: when $\lambda_1 > 0$, as long as the starting point (V_0, K_0) is close enough to the critical point (V_c, K_c) , both the tumor's volume and vasculature will tend to the critical point, which represents a fatal situation for the patient.

Additionally, as it is shown in [13, pages 5-7], what has been proved locally is also true globally: $(V(t), K(t))$ will tend to the critical point no matter where the starting point (V_0, K_0) is.

According to the Existence and Uniqueness Theorem, whose conditions are satisfied, we observe that for any initial point in $\Omega = (0, +\infty) \times (0, +\infty)$ the solution will move in concordance with the signs of V' and K' . As it can be applied all over the first quadrant, iterating this process along the points reached, we can deduce how the solution behaves globally.

The critical point (V_c, K_c) is the point where the nullclines (the curves making 0 K' and V') $K = V$ and $K = \frac{bV}{\lambda_2 + dV^{\frac{2}{3}}}$ intersect, dividing Ω into four different regions:

- i) If $K > \max \left\{ V, \frac{bV}{\lambda_2 + dV^{\frac{2}{3}}} \right\}$ then $V' > 0$ and $K' < 0$. Therefore, the solution of (2.5) will move to the right and downwards.
- ii) If $K \in \left[V, \frac{bV}{\lambda_2 + dV^{\frac{2}{3}}} \right]$ then $V' > 0$ and $K' > 0$. In this region the solution will, consequently, move to the right and upwards.
- iii) For the case in which $K < \min \left\{ V, \frac{bV}{\lambda_2 + dV^{\frac{2}{3}}} \right\}$, we get $V' < 0$ and $K' > 0$, which implies that the solution goes to the left and upwards.
- iv) When $K \in \left[\frac{bV}{\lambda_2 + dV^{\frac{2}{3}}}, V \right]$, we have $V' < 0$ and $K' < 0$, which means that the solution will move to the left and downwards.

It is important to note that, due to the fact that the Existence and Uniqueness Theorem can be applied in all the regions, whenever a solution for an initial point in regions i) or iii) reaches regions ii) or iv) it will never return to its starting region and will tend with no choice to the critical point without leaving the new region. Additionally, as it is compulsory that the solutions follow these behaviors in each region, they cannot have a negative component nor tend to $+\infty$.

This is shown in Figure 2.1, where the nullclines are represented with noncontinuous strokes; eight different initial points, with a red \star , and the parameters used are $\lambda_1 = 0.192$, $\lambda_2 = 0$, $b = 5.85$, $d = 0.00873$, which have been inspired on those from [10].

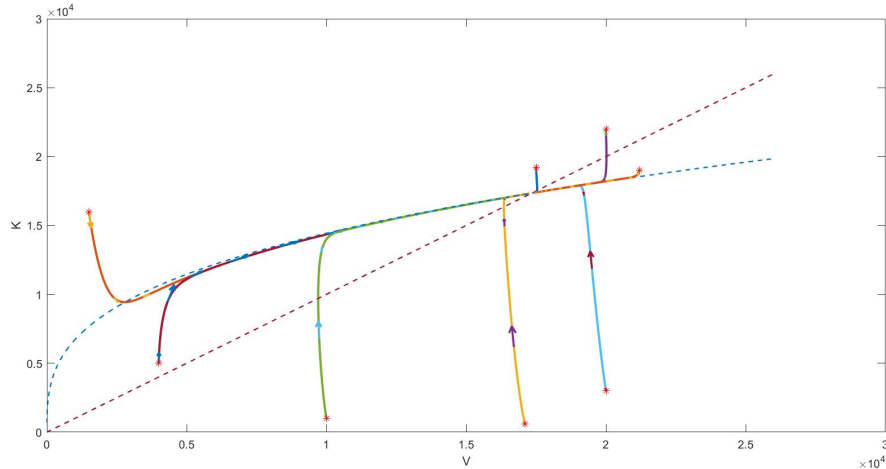


Figure 2.1: Case $\lambda_1 > 0$.

2. On the other hand, when $\boxed{\lambda_1 < 0}$, $b > \lambda_2$ implies $\lambda_1(\lambda_2 - b) > 0$, so

$$\gamma_1 = \frac{-(\lambda_1 + b)}{2} + \sqrt{\frac{2}{3}\lambda_1(\lambda_2 - b) + \left(\frac{\lambda_1 + b}{2}\right)^2} > 0,$$

$$\gamma_1 = \frac{-(\lambda_1 + b)}{2} - \sqrt{\frac{2}{3}\lambda_1(\lambda_2 - b) + \left(\frac{\lambda_1 + b}{2}\right)^2} < 0.$$

Therefore, (V_c, K_c) is not asymptotically stable anymore. Now, it is unstable. There are three different situations:

- (a) $(V_0, K_0) = (V_c, K_c)$ implies $(V(t), K(t)) \equiv (V_c, K_c)$, due to the Existence and Uniqueness Theorem.
- (b) Given $(V_0, K_0) \neq (V_c, K_c)$, $\exists(V(t), K(t))$ in $[0, T)$ for some $T < +\infty$ and $\lim_{t \rightarrow T^-} V(t) = 0$.
- (c) Given $(V_0, K_0) \neq (V_c, K_c)$, $\exists(V(t), K(t)) \forall t \geq 0$, and $\lim_{t \rightarrow +\infty} V(t) = +\infty$.

Cases 2b and 2c might be proved by observing the sign of V' and K' , which reflect how will the solution behave for initial points in the different regions provided by the nullclines (the nullclines are the same as for the case $\lambda_1 > 0$). Again, we observe that we can apply the Existence and Uniqueness Theorem iteratively with the aim of studying this behavior globally:

- i) If $K > \max \left\{ V, \frac{bV}{\lambda_2 + dV^{\frac{2}{3}}} \right\}$ then $V' < 0$ and $K' < 0$.
- ii) If $K \in \left[V, \frac{bV}{\lambda_2 + dV^{\frac{2}{3}}} \right]$ then $V' < 0$ and $K' > 0$.
- iii) If $K < \min \left\{ V, \frac{bV}{\lambda_2 + dV^{\frac{2}{3}}} \right\}$, we get $V' > 0$ and $K' > 0$.
- iv) When $K \in \left[\frac{bV}{\lambda_2 + dV^{\frac{2}{3}}}, V \right]$, then $V' > 0$ and $K' < 0$.

For an initial point (V_0, K_0) located in region i) the solution will move to the left and downwards, and if $V_0 < V_c$ then $V(t)$ will tend to 0. Instead, for some initial points with $V_0 > V_c$ the solution will change from region i) to regions iii) and iv) and $V(t)$ will tend to $+\infty$. See for example Figure 2.2: for the parameters provided, $V_c = 17347$ and for $(V_0, K_0) = (1500, 16000)$ and $(V_0, K_0) = (17500, 19200)$, $V(t)$ tends to 0. Instead, for $(V_0, K_0) = (20000, 22000)$, it tends to $+\infty$.

For initial points in region ii), the solution will move to the left and upwards and once the solution finds itself in region i) it will behave as mentioned above

for the cases with $V_0 < V_c$, without coming back to region ii) (see for example $(V_0, K_0) = (4000, 5000)$ in Figure 2.2).

In region iii) the solution goes to the right and upwards. We can distinguish two cases: it reaches region ii), and then it behaves as we have just explained ($(V_0, K_0) = (10000, 1000)$ in Fig. 2.2), or $V(t)$ tends to $+\infty$ (see $(V_0, K_0) = (17100, 600)$ and $(V_0, K_0) = (20000, 3000)$).

For initial points in region iv) the solution moves to the right and downwards, and may change to region iii), and act as it did for the cases in which $V(t)$ tended to $+\infty$ (see $(V_0, K_0) = (21200, 19000)$).

We include here Figure 2.2, where $\lambda_1 = -2$, $\lambda_2 = 0$, $b = 5.85$, $d = 0.00873$ and the initial points are represented with a green \circ for the cases in which $V(t)$ tends to 0 and a red \star for those in which it tends to $+\infty$.

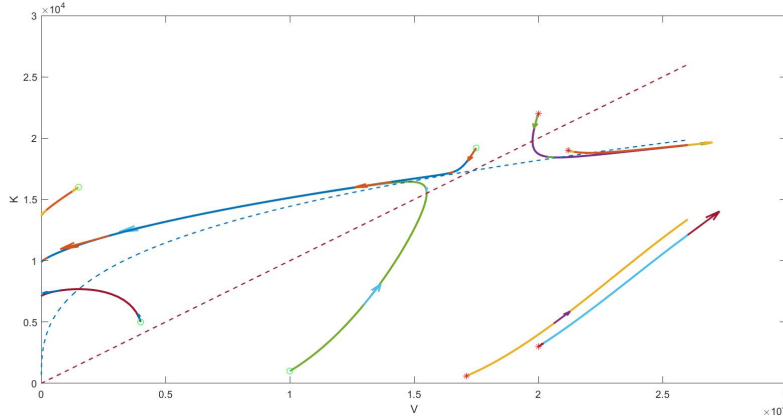


Figure 2.2: Case $\lambda_1 < 0$

For these parameters, as we have shown, depending on the initial points, $V(t)$ will tend to $+\infty$ or to 0. Therefore, we include the next figure to show for which initial points the volume of the tumor would tend to 0 and for which it would grow infinitely. This did not happen in the former case, with $\lambda_1 > 0$, where the solution moved towards the critical point independently of the initial point.

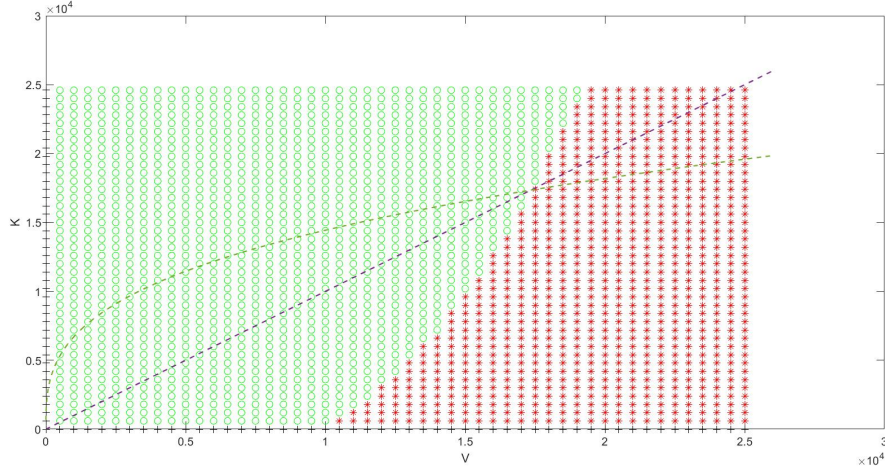


Figure 2.3: Initial points. Case $\lambda_1 < 0$. \star if $V(t)$ tends to $+\infty$, \circ if it tends to 0.

We have observed, mathematically, that in $(0, V_c) \times (0, K_c)$ we can distinguish two cases depending on the initial point (V_0, K_0) (for $\lambda_1 < 0$ and $b > \lambda_2$):

- When $V_0 > K_0$ (this is, under the diagonal) the volume of the tumor can grow infinitely or, instead, it can decrease as time goes by.
- For any initial point with $V_0 < K_0$ then the volume will tend to 0.

These events will be discussed in the next chapter.

Case $b \leq \lambda_2$: Now, the problem does not have a critical point. This is, the nullclines no longer intersect in $(0, +\infty) \times (0, +\infty)$ and now they divide Ω into 3 regions. We can follow the same reasoning as for $b > \lambda_2$ and study the sign of the derivatives in each of them to deduce how the solution behaves globally because the Existence and Uniqueness Theorem can be used in all the points of the first quadrant.

1. If $\lambda_1 > 0$ the solution will tend to the origin when $t \rightarrow +\infty$ independently of the region where the starting point is located:
 - i) If $K > V$ then $V' > 0$ and $K' < 0$ and the solution will move to the right and downwards.
 - ii) If $K \in \left[\frac{bV}{\lambda_2 + dV^{\frac{2}{3}}}, V \right]$ then $V' < 0$ and $K' < 0$ and it will move to the left and downwards.
 - iii) If $K < \frac{bV}{\lambda_2 + dV^{\frac{2}{3}}}$, we get $V' < 0$ and $K' > 0$, which implies that the solution goes to the left and upwards.

For initial points in regions i) or iii) the solution may cross the nullclines and remain in region ii) while it moves to the left and downwards.

This case is presented in [13, page 8], where it is explained that, again, the solutions cannot tend to infinity nor to another quadrant, and we show it in Figure 2.4, where $\lambda_1 = 0.192$, $\lambda_2 = 0.3$, $b = 0.2$, $d = 0.00873$. These parameters have been inspired on the ones taken in [10], although b and λ_2 have been modified in order to accomplish $b \leq \lambda_2$. This is an academic case, since usually we will have $\lambda_2 = 0$. We have chosen, for this figure, other initial points in order to consider at least one of each region.

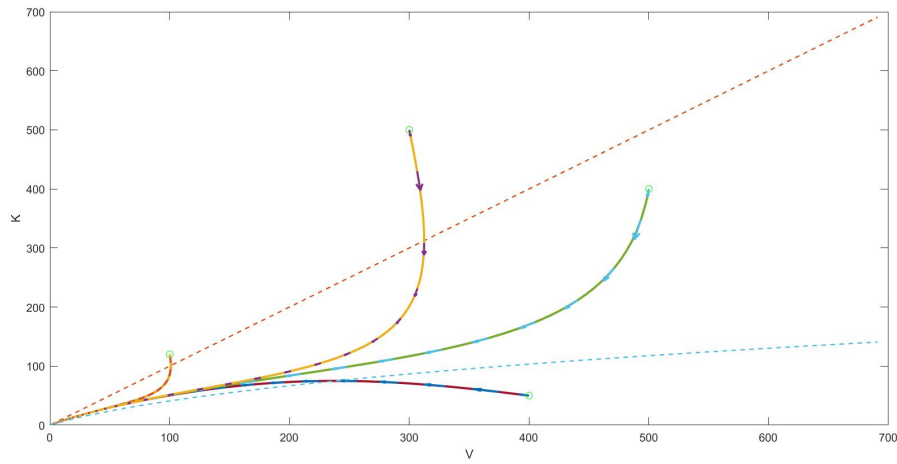
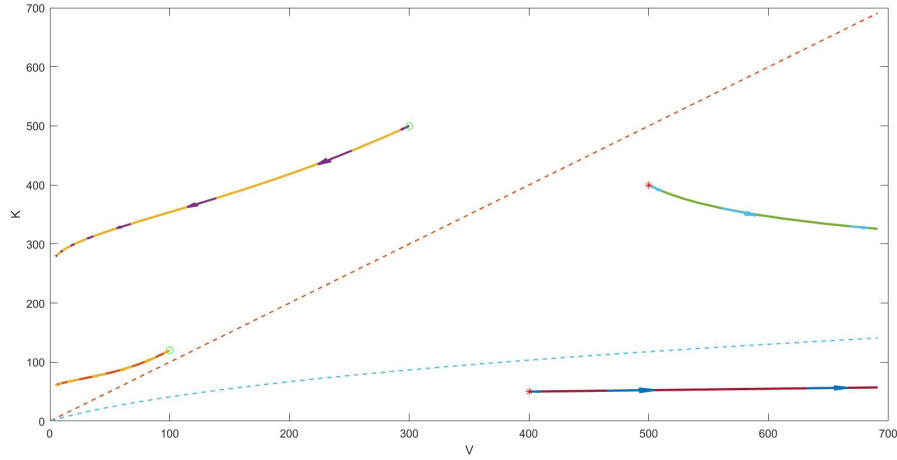


Figure 2.4: Case $\lambda_1 > 0$

2. Instead, when $\lambda_1 < 0$, either $\lim_{t \rightarrow T^-} V(t) = 0$ or $\lim_{t \rightarrow +\infty} V(t) = +\infty$:

- i) If $K > V$ then $V' < 0$ and $K' < 0$ and the solution will move to the left and downwards.
- ii) If $K \in \left[\frac{bV}{\lambda_2 + dV^{2/3}}, V \right]$ then $V' > 0$ and $K' < 0$ which means that the solution goes to the right and downwards.
- iii) If $K < V$ then $V' > 0$ and $K' > 0$, and therefore it moves to the right and upwards.

This can be seen in Figure 2.5 for $\lambda_1 = -2$, $\lambda_2 = 0.3$, $b = 0.2$, $d = 0.00873$.

Figure 2.5: Case $\lambda_1 < 0$

We include here a table resuming what was explained before:

	$b > \lambda_2$	$b \leq \lambda_2$
$\lambda_1 > 0$	$\lim_{t \rightarrow +\infty} (V(t), K(t)) = (V_c, K_c)$	$\lim_{t \rightarrow +\infty} (V(t), K(t)) = (0, 0)$
$\lambda_1 < 0$	(2a) $(V(t), K(t)) \equiv (V_c, K_c)$ (2b) $\lim_{t \rightarrow T^-} V(t) = 0$ (2c) $\lim_{t \rightarrow +\infty} V(t) = +\infty$	$\lim_{t \rightarrow T^-} V(t) = 0$ $\lim_{t \rightarrow +\infty} V(t) = +\infty$

Table 2.1: Different situations depending on the values of the parameters λ_1 , b and λ_2 .

2.3 Hahnfeldt model variant with logistic

As we commented before, the logistic model is also used in biology to study tumors' growth. Its ODE was described in (2.2) and we will consider again a dynamic carrying capacity, $K(t)$, described in (2.4). With all this taken into account, the ODE system would be:

$$\begin{cases} V'(t) = \lambda_1 V(t) \left(1 - \frac{V(t)}{K(t)}\right) & \text{with } V(0) = V_0 > 0, \\ K'(t) = -\lambda_2 K(t) + bV(t) - dK(t)V^{2/3}(t) & \text{with } K(0) = K_0 > 0, \end{cases}$$

whose associated autonomous system would be:

$$\begin{cases} V' = \tilde{f}_1(V, K), \\ K' = \tilde{f}_2(V, K). \end{cases} \quad (2.7)$$

Clearly, it is necessary that $V = K$ so as to get $\tilde{f}_1(V, K) = 0$ and the point that makes $\tilde{f}_2(V, K) = 0$ at the same time is $(\tilde{V}_c, \tilde{K}_c)$ with $\tilde{V}_c = \tilde{K}_c = \left(\frac{b - \lambda_2}{d}\right)^{3/2}$, considering $b > \lambda_2$. Thus, the critical point using the logistic model is the same as the one that we got using the Gompertz's one.

To study, locally, the stability of the system we will take the Taylor's formula of \tilde{f}_1 and \tilde{f}_2 at $\tilde{V}_c = \tilde{K}_c$ and we will linearize them to rewrite (2.7):

Denoting $x := V - \tilde{V}_c$ and $y := K - \tilde{K}_c$,

$$\begin{pmatrix} x' \\ y' \end{pmatrix} = \underbrace{\begin{pmatrix} -\lambda_1 & \lambda_1 \\ \frac{b + 2\lambda_2}{3} & -b \end{pmatrix}}_A \begin{pmatrix} x \\ y \end{pmatrix} \quad (2.8)$$

where the eigenvalues of matrix A are those obtained for the Gompertzian growth model. Therefore, the local conclusions for the critical point ($b > \lambda_2$) deduced are the same for both models:

- When $\lambda_1 > 0$ we face an asymptotically stable case: both eigenvalues are negative, which implies that for any starting point close enough to the critical point, the volume and the vasculature will tend to the critical point.
- An opposite situation occurs when $\lambda_1 < 0$: the critical point is no longer stable but an unstable point, and the volume and the vasculature will not necessarily tend to it.

Globally, when $b > \lambda_2$ and when $b \leq \lambda_2$, the solutions behave as they did, respectively, when considering the Hahnfeldt's model. We can say that for this model the global analysis remains the same as for the other one, being it resumed in Table 2.1.

Chapter 3

PK/PD

“In simple terms pharmacokinetics may be viewed as what the body does to the drug, and pharmacodynamics as what the drug does to the body” is the description we can find in [16]. This is the most intuitive way of understanding these two concepts, which play a major role in pharmacology. Both pharmacokinetics (PK) and pharmacodynamics (PD) will be considered in this chapter, for the case on which drugs are administered to a body with a tumor.

3.1 Pharmacokinetics

When a drug is injected into a body, it would be reasonable to expect it to be distributed in a proportional way all around the bloodstream. Nevertheless, what does happen is not this: it has been observed that the drug is absorbed by other organs and tissues, being its blood concentration reduced. The volume of distribution, V_D , relates drug amount in the body with its concentration in plasma (see [20]), and its units can be L or L/kg.

How the body absorbs drugs is one of the main subjects of study of pharmacokinetics, but there are more: drug distribution, metabolism and excretion. In order to predict drug behavior, different models are used. We can distinguish between non-compartmental models and compartmental ones (see [1]). Here, we will consider a mono-compartmental model.

As it was done in [8], we will use the following first-order Cauchy problem to describe the concentration of the drug in the body:

$$\begin{cases} c'(t) = -\lambda c(t) + u(t), \\ c(0) = 0, \end{cases} \quad (3.1)$$

where λ is the elimination rate constant and $u(t)$ is a generalised function that depends on which drug is administered and how. In this work, as it was done in the cited one,

we will consider that the drug is given via injections in N doses $\{d_i\}_{i=1}^N$, and that it will spread throughout the whole body instantaneously (mono-compartmental model). We will assume that the injections take place at times $0 \leq t_1 < t_2 < \dots < t_N$ respectively.

We describe $u(t)$ as follows:

$$u(t) = \sum_{i=1}^N \sigma d_i \delta(t - t_i), \quad (3.2)$$

being $\delta(t - t_i)$ the Dirac delta distribution concentrated at t_i .

As we have mentioned, $u(t)$ not only depends on the drug but also on its administration. The body surface area (BSA), which we will be calling α , is a determinant factor on how drugs are administered, as well as the patient's weight (kg), β . σ in (3.2) will take different expressions according on how the units of the doses d_i are given in order to keep consistency in terms of units (concentration is usually given as $\frac{\text{mg}}{\text{L}}$):

Doses units	Expression for σ	Where...
$\frac{\text{mg}}{\text{kg}}$	$\frac{\beta}{V_D} \text{kg/L}$	β is given in kg and V_D in L.
$\frac{\text{mg}}{\text{m}^2}$	$\frac{\alpha}{V_D} \text{m}^2/\text{L}$	α is given in m^2 and V_D in L.
	$\frac{\alpha}{V_D \beta} \text{m}^2/\text{L}$	α is given in m^2 , β in kg and V_D in L/kg.

Table 3.1: Different expressions for σ in (3.2) for the two typical units in which doses d_i are given.

The problem (3.1) can be rewritten as:

$$\begin{cases} c'(t) = -\lambda c(t) + \sum_{i=1}^N \sigma d_i \delta(t - t_i) \\ c(0) = 0, \end{cases} \quad (3.3)$$

whose solution, considering the derivatives in the distributions sense, is given in [8] as:

$$c(t) = \begin{cases} 0 & t \in [0, t_1), \\ \sigma e^{-\lambda t} d_1 e^{\lambda t_1} & t \in [t_1, t_2), \\ \sigma e^{-\lambda t} (d_1 e^{\lambda t_1} + d_2 e^{\lambda t_2}) & t \in [t_2, t_3), \\ \vdots & \vdots \\ \sigma e^{-\lambda t} (d_1 e^{\lambda t_1} + d_2 e^{\lambda t_2} + \dots + d_{N-1} e^{\lambda t_{N-1}}) & t \in [t_{N-1}, t_N), \\ \sigma e^{-\lambda t} (d_1 e^{\lambda t_1} + d_2 e^{\lambda t_2} + \dots + d_N e^{\lambda t_N}) & t \in [t_N, T_F). \end{cases} \quad (3.4)$$

It is clear that $c(t)$ is not continuous at t_i for $i = 1, \dots, N$. Nonetheless, it is continuous in each interval. The Heaviside function, whose derivative in the sense of distributions is the Dirac delta, can be used to describe this phenomenon. This is because we have considered that, at the instant of the administration, the drug spreads instantaneously all over the body and, therefore, we will find a jump discontinuity at each moment t_i . With the intention of simplifying the expressions, we will take $\sigma = 1$. If we want to study the general case, without this simplification, then σd_i should take the place of d_i in what follows.

3.2 Pharmacodynamics

In Chapter 2, we presented some equations that could help us to model the evolution of both the volume and the vasculature of tumors. Now, we will reformulate them to make them useful for perturbed situations, where a drug is administered. Different effects can be purchased when it comes to tumors: we may want the drug to act directly on the tumor volume (V), which is known as cytotoxic effect, and an antiangiogenic one, when we want it to affect the vasculature (K). Additionally, a cytotoxic antiangiogenic effect can be another objective of drug administration.

3.2.1 Cytotoxic effect

Let $V'(t) = I(t)V(t)$ be the ODE describing the tumor growth for a non-perturbed case, being $I(t)$ a function depending on the model (for example, for the Gompertzian model we would have $I(t) = -\lambda_1 \log \left(\frac{V(t)}{K(t)} \right)$, as we have shown in (2.3)).

Historically, the drug's cytotoxic effects have been represented by adding an additional term, $-\mu V(t)c(t)$, to the ODE, which means that the effect of the drug is considered to be related to the volume of the tumor, but independent of how it grows in the non-perturbed case. A new point of view was firstly proposed by L. Norton and R. Simon (see [12]).

Using the hypothesis of [12], with the notation of our work, the anti-tumor influence of the drug would be reflected by the appearance of a multiplying factor $\alpha(t)$ in the ODE. In other words, under the effect of the drug we would have $V'(t) = I(t)V(t)\alpha(t)$, where the expression of $\alpha(t)$ may vary depending on the model chosen for the level of therapy.

The Emax model, for which $\alpha(t) = 1 - \frac{k_1 c(t)}{k_2 + c(t)}$, considers that the drug's effect is bounded. Constants $k_1 > 0$ and $k_2 > 0$ are experimentally estimated and represent, respectively, the maximum effect of the drug on the body and the effective concentration (concentration producing 50% of the maximum effect, also known as $EC50$):

As we are assuming that the concentration effect is given by $\frac{k_1 c(t)}{k_2 + c(t)}$, we observe that $\lim_{c \rightarrow +\infty} \frac{k_1 c}{k_2 + c} = k_1$, which means that k_1 is, indeed, the maximum effect of the drug on the body. At the same time, if we want to calculate the concentration producing 50% of the maximum effect, which is $\frac{k_1}{2}$, we get $\frac{k_1 c}{k_2 + c} = \frac{k_1}{2}$ if $c = k_2$, as we have just said (see [8]). We will use this model since drug resistance has been observed for cytotoxic treatments.

3.2.2 Antiangiogenic effect

The drug effects are now observable at the vasculature rather than at the tumor itself. Thereby, we must change (2.4) to take into account the effect of this kind of drugs:

$$K'(t) = -\lambda_2 K(t) + bV(t) - dK(t)V^{2/3}(t) - eK(t)c(t), \quad (3.5)$$

where $c(t)$ is the concentration of drug at time t and $e > 0$, the factor quantifying its consequences on the carrying capacity (see [10]). Note that in this case the drug's effect is not bounded.

3.2.3 Cytotoxic antiangiogenic effect

If we combine what we have just mentioned, we can formulate an ODE system to include the effect of the drug on the volume and the vasculature. Firstly, we will do it for the Gompertzian model, although we will deal with the logistic one later.

Now, the ODE system would be:

$$\begin{cases} V'(t) = -\lambda_1 V(t) \log \left(\frac{V(t)}{K(t)} \right) \left(1 - \frac{k_1 c(t)}{k_2 + c(t)} \right) & \text{with } V(0) = V_0 > 0, \\ K'(t) = -\lambda_2 K(t) + bV(t) - dK(t)V^{2/3}(t) - eK(t)c(t), & \text{with } K(0) = K_0 > 0, \end{cases} \quad (3.6)$$

Although its parameters have already been presented, we will make a point: physically, λ_1 is the growth rate and it should be positive. Therefore, now $\lambda_1 > 0$. The reason why we let it take negative values in the former chapter will be explained soon.

It is important to note that if we want to use a cytotoxic antiangiogenic treatment then $k_1, e \neq 0$. If we consider that the drug will only affect the tumor (cytotoxic, non-antiangiogenic drug) then $k_1 \neq 0, e = 0$ and for the opposite case, when the drug only has effects on the vasculature but not on the tumor, then $k_1 = 0, e \neq 0$.

Constant concentration

Aiming to study the behavior of the solution we will, firstly, distinguish the case on which $c(t) \equiv c_d > 0$ constant. Now, $\alpha(t) \equiv \alpha_d = 1 - \frac{k_1 c_d}{k_2 + c_d}$ and we can write the next

autonomous system:

$$\begin{cases} V' = \hat{f}_1(V, K) = -\lambda_1 V \log\left(\frac{V}{K}\right) \alpha_d, \\ K' = \hat{f}_2(V, K) = -\lambda_2 K + bV - dKV^{2/3} - eKc_d, \\ V(0) = V_0 > 0, K(0) = K_0 > 0. \end{cases} \quad (3.7)$$

It is noteworthy that we will consider that $\alpha_d \lambda_1$ takes the place of λ_1 in Chapter 2, and α_d can take negative values if $c_d > \frac{k_2}{k_1 - 1}$ and $k_1 > 1$. This is why we allowed λ_1 to take negative values in that chapter. α_d being positive can be due to the nature of the drug (non-cytotoxic, so $k_1 = 0$) or to not a sufficient amount of drug being administered. This is, when $c_d < \frac{k_2}{k_1 - 1}$ (the level of concentration is under a certain value), with $k_1 > 1$, then α_d takes positive values.

Following the reasoning of Chapter 2, we calculate a critical point for (3.7). We make $V = K$ in order to get $\hat{f}_1(V, K) = 0$ and, substituting in $\hat{f}_2(V, K)$, we obtain that (as $V > 0$) a critical point for (3.7) is (\hat{V}_c, \hat{K}_c) with $\hat{V}_c = \hat{K}_c = \left(\frac{b - ec_d - \lambda_2}{d}\right)^{\frac{3}{2}}$.

We get the same results as in the former chapter with a slight difference: $\lambda_2 + ec_d$ will take the place of λ_2 (see Table 2.1).

	$b > \lambda_2 + ec_d$	$b \leq \lambda_2 + ec_d$
$c_d < \frac{k_2}{k_1 - 1}$	$\lim_{t \rightarrow +\infty} (V(t), K(t)) = (\hat{V}_c, \hat{K}_c)$	$\lim_{t \rightarrow +\infty} (V(t), K(t)) = (0, 0)$
$c_d > \frac{k_2}{k_1 - 1}$	$(V(t), K(t)) \equiv (\hat{V}_c, \hat{K}_c)$ $\lim_{t \rightarrow T^-} V(t) = 0$ $\lim_{t \rightarrow +\infty} V(t) = +\infty$	$\lim_{t \rightarrow T^-} V(t) = 0$ $\lim_{t \rightarrow +\infty} V(t) = +\infty$

Table 3.2: Different situations depending on the values of the parameters c_d , b and $\lambda_2 + ec_d$, with $k_1 > 1$.

Note that the results of Table 3.2 can also be applied for a cytotoxic non-antiangiogenic treatment, characterised by $e = 0$; and for an only antiangiogenic treatment, where $\alpha_d = 1 > 0$ (as $k_1 = 0$).

As it is shown in this table, the solutions behave on different ways depending on the parameters:

- If $\alpha_d > 0$ ($c_d < \frac{k_2}{k_1 - 1}$), the solution will tend to the critical point, which exists if $b > \lambda_2 + ec_d$, or to the origin, if it does not exist.

- Likewise, if $c_d > \frac{k_2}{k_1 - 1}$, with $k_1 > 1$, then $\alpha_d < 0$. Here we will distinguish different cases:
 - If the critical point exists ($b > \lambda_2 + ec_d$):
 - * If the critical point is the initial point, the solution will be constant and will take the value of the critical point.
 - * If $V_0 < K_0 < \hat{V}_c = \hat{K}_c$ then $V(t)$ will tend to 0.
 - * If $K_0 < V_0 < \hat{V}_c = \hat{K}_c$ then the initial point plays a major role on how the solution behaves, and $V(t)$ can tend either to 0 or to $+\infty$.
 - When it does not exist, this is, when $b \leq \lambda_2 + ec_d$:
 - * If $V_0 < K_0$ then $V(t)$ will tend to 0.
 - * The volume will tend to $+\infty$ if $K_0 < V_0$.

We include some figures for initial points fulfilling $K_0 < V_0$ to make it easier to understand what we have just explained. We will start by the last case, $b \leq \lambda_2 + ec_d$, as its discussion is shorter than the one of $b > \lambda_2 + ec_d$.

- $b \leq \lambda_2 + ec_d$: In Figure 3.1 we show how, for the same initial points, different values of c_d (and therefore, different values of α_d) lead to different situations. Graphics in the same row have the same initial point but different concentrations, whereas graphics in the same column have the same concentration but different initial points. As we did in Chapter 2 for the case $b \leq \lambda_2$, the parameters have been slightly modified to explain this case.

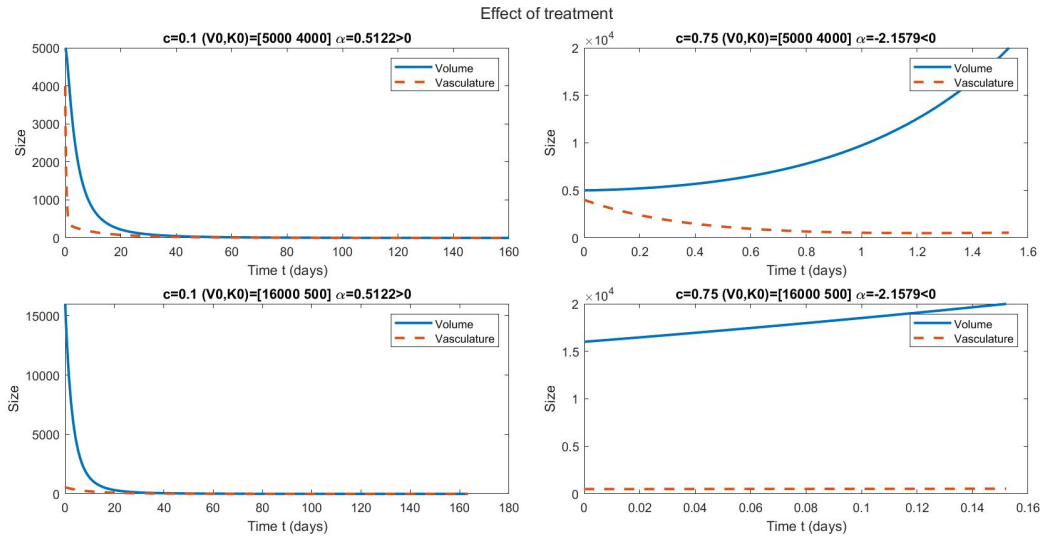


Figure 3.1: $\lambda_1 = 0.192$, $\lambda_2 = 0.3$, $b = 0.2$, $d = 0.00873$, $e = 0$, $k_1 = 20$, $k_2 = 4$

We observe that, when $c_d < \frac{k_2}{k_1 - 1}$ ($\alpha_d > 0$, see the 1st column), regardless of the initial point (with $K_0 < V_0$), the volume $V(t)$ tends to 0 whereas it tends to $+\infty$ when $\alpha_d < 0$.

In a VK portrait, Figure 3.1 would look as follows:

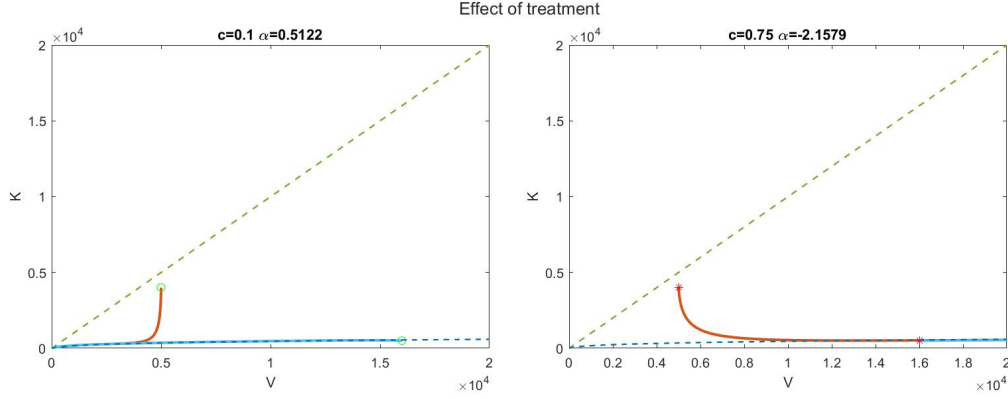


Figure 3.2: VK portraits for Figure 3.1

- $b > \lambda_2 + ec_d$: We repeat the same experiment but with some parameters for which this inequality is true. In Figure 3.3 the graphics are distributed as in Figure 3.1. We can observe that, for the same concentration but depending on the initial point, when $\alpha_d > 0$ then the solution tends to the critical point (1st column), and that the volume may tend to 0 or grow indefinitely if $\alpha_d < 0$ (see the 2nd column).

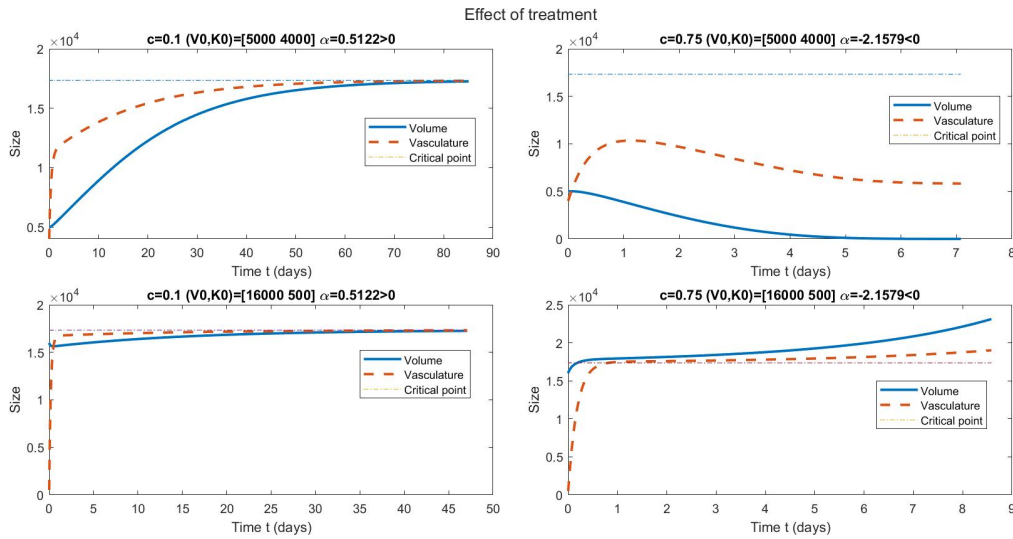


Figure 3.3: Parameters: $\lambda_1 = 0.192$, $\lambda_2 = 0$, $b = 5.85$, $d = 0.00873$, $e = 0$, $k_1 = 20$, $k_2 = 4$.

The VK portraits will now look like those in Figure 3.4.

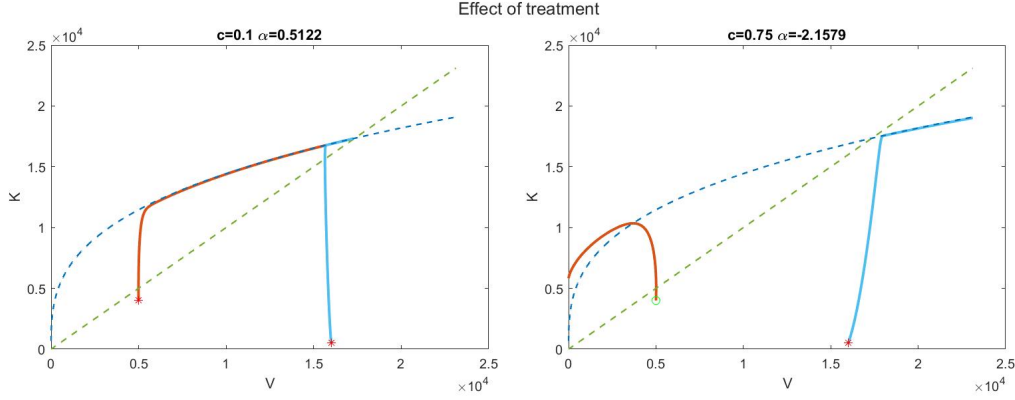


Figure 3.4: VK portraits for Figure 3.3

Looking at the second columns of the last 4 figures, we observe a striking and (apparently) contradictory situation: when applying drug to the tumor whose initial conditions fulfill $V_0 > K_0$, we expect its volume to get nullified. Nevertheless, we notice that, in some cases, it can grow indefinitely. In the second columns of Figures 3.3 and 3.4, we appreciate how, if $b > \lambda_2 + ec_d$, this can take place or not depending on the initial point.

We had already noticed this counter intuitive fact in the former chapter, for the case $\lambda_1 < 0$ and $b > \lambda_2$ (as this situation takes place in spite of whether $e = 0$ or not). We included a graphic (see Figure 2.3, corresponding to $\lambda_1 \alpha_d = -2$) that showed that this fact is not only conditioned by the initial volume but also by the initial value of the vasculature K_0 . We will, therefore, distinguish two sections in our VK portraits, the normal one, where the volume behaves as expected when administering a drug, and the abnormal one, where it grows indefinitely. This abnormal region is the one marked with \star . Biologically, this paradoxical case has also been observed, and different medical explanations have been given aiming to explain it, as we will show in the last chapter.

Non-constant concentration

It seems pertinent to consider the case where $c(t)$ is not constant, as the resemblances between the constant and the non-constant cases may not be obvious, and, as we have already mentioned, drug concentration in the body may vary within time.

Theorem 3.2.1. *Let $K_0 > 0$ and $V_0 > 0$ and let $c : [0, +\infty) \rightarrow [0, +\infty)$ be a piecewise continuous function with a finite number of jump discontinuities. Then, (3.6) has a unique solution $(V(t), K(t))$ which*

- is defined in $[0, +\infty)$,
- or is defined in $[0, T)$ for some $T > 0$ and it is verified $V(t) \rightarrow 0$ when $t \rightarrow T^-$.

Proof. Firstly, we will demonstrate the existence and uniqueness of solution for each interval where $c(t)$ is continuous. We will consider the interval $[0, t_1)$, but the proof follows the same reasoning for the intervals $[t_i, t_{i+1})$, with $i \in \{1, \dots, N-1\}$, and for $[t_N, T_F)$.

We have assumed that the initial point $(V(0), K(0)) = (V_0, K_0) \in \Omega$, where $\Omega = (0, +\infty) \times (0, +\infty)$, as we said in the former chapter. Let

$$\begin{aligned}\hat{f}_1(t, V, K) &= -\lambda_1 V \log \left(\frac{V}{K} \right) \left(1 - \frac{k_1 c(t)}{k_2 + c(t)} \right); \\ \hat{f}_2(t, V, K) &= -\lambda_2 K + bV - dKV^{2/3} - eKc(t).\end{aligned}$$

We need to prove that both $\hat{f}_1(t, V, K)$ and $\hat{f}_2(t, V, K)$ are continuous and have partial derivatives continuous in $[0, t_1) \times \Omega$ in order to demonstrate the local existence and uniqueness of solution. It is clear that they are continuous there because $-\lambda_1 V \log \left(\frac{V}{K} \right)$ and $\lambda_2 K + bV - dKV^{2/3}$ are continuous in Ω and $c(t)$ is continuous when $t \in [0, t_1)$. We observe that this is true regardless of whether e and k_1 are 0 or not.

The partial derivatives are, calling $1 - \frac{k_1 c(t)}{k_2 + c(t)} = \alpha(t)$:

$$\begin{aligned}\frac{\partial \hat{f}_1}{\partial V}(t, V, K) &= -\lambda_1 \alpha(t) \left(\log \left(\frac{V}{K} \right) - 1 \right) & \frac{\partial \hat{f}_1}{\partial K}(t, V, K) &= \lambda_1 \frac{V}{K} \alpha(t) \\ \frac{\partial \hat{f}_2}{\partial V}(t, V, K) &= b - \frac{2}{3} dKV^{-1/3} & \frac{\partial \hat{f}_2}{\partial K}(t, V, K) &= -\lambda_2 - dV^{2/3} - ec(t)\end{aligned}$$

and, again, it is clear that they are continuous in $[0, t_1) \times \Omega$. Thereby, we can say that, for some $h \in (0, t_1)$, there exists a solution for each (V_0, K_0) and it is defined in $[0, h]$. Now, we will have to distinguish two cases:

- On one hand, when $\alpha(t) > 0$, as we have seen in the former chapter for $\lambda_1 > 0$, the solution does not tend to Ω 's boundary nor diverges. Since, therefore, $(V(h), K(h)) \in \Omega$, and we know that $c(t)$ is continuous in $[0, t_1)$, we can iterate the process and we will have proved the existence and uniqueness of a solution in $t \in [0, t_1)$. This reasoning must be followed for the other intervals too.

The example given in [13, pages 10, 11] illustrates that, as $V'(t)$ and $K'(t)$ are piecewise continuous with respect to t and C^1 with respect to V and K , we can

extend the existence and uniqueness of solution that has been proved for each interval to the entire interval $[0, +\infty)$.

Note that, in this case, the existence and uniqueness of solution is not affected by whether $e = 0$ or not. Instead, what does have an influence on the existence and uniqueness of solution is the term referring to the cytotoxic treatment. If the drug administered is not expected to have a direct effect on the tumor (or not a sufficient amount is provided) then we will have $\alpha(t) > 0$ and we will be able to affirm that there exists a solution for (3.6) defined in $[0, +\infty)$ and that it is unique.

- On the other hand, when $\alpha(t)$ takes negative values, we can no longer use the same argument: we can not state that the solution does not tend to Ω 's boundaries, as studying the sign of V' and K' in different regions we observe that for some initial points then $(V(t), K(t))$ tends to the left and downwards, getting close to the second quadrant (see the constant case for $\alpha_d < 0$, or Figures 2.2 and 2.5 of the former chapter). Now, as $V(t) \rightarrow 0$ when $t \rightarrow T^-$ for some $T > 0$, we will only be able to affirm that $(V(h), K(h)) \in \Omega$ (h may vary after each iteration) a limited number of times.

We can then apply the argument of [13], pasting the solutions at the points where $c(t)$ has discontinuities, but only for some intervals, until we get to prove the existence and uniqueness of solution in $[0, T)$ for some $T > 0$.

Here again, both cases $e = 0$ and $e \neq 0$ lead us to the same conclusions as far as $\alpha(t) < 0$, which depends on the drug.

□

We can follow the same reasoning for the **logistic model**. Now, we write (3.6) with the equation given by this model:

$$\begin{cases} V'(t) = \lambda_1 V(t) \left(1 - \frac{V(t)}{K(t)}\right) \left(1 - \frac{k_1 c(t)}{k_2 + c(t)}\right) & \text{with } V(0) = V_0 > 0, \\ K'(t) = -\lambda_2 K(t) + bV(t) - dK(t)V^{2/3}(t) - eK(t)c(t), & \text{with } K(0) = K_0 > 0, \end{cases} \quad (3.8)$$

and, again, $\lambda_1 > 0$ due to the biological reasons already explained and k_1 and e will be 0 or not depending on the treatment.

Constant concentration - Logistic model

As happened in the previous chapter, the conclusions obtained when using the logistic model are the same as the ones that were deduced for the Gompertzian model.

Non-constant concentration - Logistic model

For a non-constant concentration, we can repeat the arguments followed for the other model and we can state Theorem 3.2.1 for (3.8) instead of (3.6). Its proof remains essentially the same, as now the partial derivatives of

$$\begin{aligned}\hat{f}_1(t, V, K) &= \lambda_1 V \left(1 - \frac{V}{K}\right) \left(1 - \frac{k_1 c(t)}{k_2 + c(t)}\right) \text{ and} \\ \hat{f}_2(t, V, K) &= -\lambda_2 K + bV - dKV^{2/3} - eKc(t)\end{aligned}$$

are

$$\begin{aligned}\frac{\partial \hat{f}_1}{\partial V}(t, V, K) &= \lambda_1 \alpha(t) \left(1 - \frac{2V}{K}\right) & \frac{\partial \hat{f}_1}{\partial K}(t, V, K) &= \lambda_1 \frac{V^2}{K^2} \alpha(t) \\ \frac{\partial \hat{f}_2}{\partial V}(t, V, K) &= b - \frac{2}{3} dKV^{-1/3} & \frac{\partial \hat{f}_2}{\partial K}(t, V, K) &= -\lambda_2 - dV^{2/3} - ec(t)\end{aligned}$$

which are continuous in the same regions as the ones of the Gompertzian model.

3.3 Keeping concentration near a constant value

Having $c(t) \equiv c_d$ is a Utopian situation because, as we have already explained in Section 3.1, the drug undergoes different biological processes that affect its concentration in the body, such as metabolism or excretion.

Nevertheless, we may want to keep the concentration level as constant as possible. We observe that the stabilization of $c(t)$ and the one of $\frac{k_1 c(t)}{k_2 + c(t)}$ are highly related: considering that there exists another constant, k_3 , such that $0 \leq c(t) \leq k_3$, we have that

$$\begin{aligned}\frac{k_1 k_2 |c(t) - c_d|}{(k_2 + k_3)(k_2 + c_d)} &\leq \left| \frac{k_1 c(t)}{k_2 + c(t)} - \frac{k_1 c_d}{k_2 + c_d} \right| = \\ &= \left| \frac{k_1 c(t)(k_2 + c_d) - k_1 c_d(k_2 + c(t))}{(k_2 + c(t))(k_2 + c_d)} \right| \leq \frac{k_1 |c(t) - c_d|}{k_2 + c_d}.\end{aligned}\tag{3.9}$$

This is, stabilizing $c(t)$ stabilizes $\frac{k_1 c(t)}{k_2 + c(t)}$ and vice-versa. We will take this into account in the next chapter, aiming to find the parameters that keep $\frac{k_1 c(t)}{k_2 + c(t)}$ as constant as possible.

Chapter 4

Computational experiments

For this chapter, we will focus on the case $b > \lambda_2$, which gives us a critical point (V_c, K_c) , as we have explained before. This critical point represents a fatal situation for the patient and, therefore, the region that we will be considering is $(0, V_c) \times (0, K_c)$, in order to study only these situations in which the patient is still alive. Aiming to do so, we will carry out some experiments, for which we will need to give some values to the different parameters presented in the previous chapters, being some of them determined by the type of tumor and the drug applied. In addition, we will try to choose the parameters N, d_i, t_i in (3.3) that maintain $c(t)$ as close as possible to a desired constant c_d in order to keep the expression $\frac{k_1 c(t)}{k_2 + c(t)}$ as constant as possible. We will use MATLAB, being resumed the functions we have used in Section 4.4.

4.1 Parameters

We will start by introducing the abbreviation AUC: “Area Under the Curve”. AUC is usually used to measure the degree of exposure to the drug and to compare drugs’ bio-availability. We can calculate it as follows:

$$\int_0^{T_F} c(t) dt. \quad (4.1)$$

Nevertheless, although AUC is the most habitual comparison criteria for treatments, sometimes we can also find that they are compared in base to the total administered drug:

$$\int_0^{T_F} u(t) dt, \quad (4.2)$$

being $u(t)$ the one in (3.1).

We will be using (4.1) and (4.2) to calculate the parameters needed. Firstly, we will consider that the concentration of the drug takes a constant value $c(t) \equiv c_d$. From (3.1) we deduce $u(t) = \lambda c_d$, which corresponds to a constant infusion. In this case, if we calculate the AUC, we get that $\int_0^{T_F} c(t) dt = c_d T_F$. Additionally, $\int_0^{T_F} u(t) dt = \lambda c_d T_F$.

Now, we take the general expressions for $c(t)$ and $u(t)$ in the discrete case. These expressions are the ones in (3.3) and (3.2). Taking $t_1 = 0$, $t_N < T_F$, we calculate the AUC and (4.2), getting

$$\int_0^{T_F} c(t) dt = \frac{1}{\lambda} \sum_{i=1}^N \sigma d_i (1 - e^{\lambda(t_i - T_F)}) \quad (4.3)$$

(see [13]) and

$$\int_0^{T_F} u(t) dt = \sigma \sum_{i=1}^N d_i. \quad (4.4)$$

4.1.1 Equispaced administration times

For simplicity, we will consider that the administration times are equispaced, and that the doses are all the same; this is, $t_{i+1} - t_i = \Delta$ for $i = 1, \dots, N-1$ and $d_i = \hat{d}$ for $i = 1, \dots, N$, and $N\Delta = T_F$.

Taking this into account, we reformulate (4.3) and (4.4) to have:

$$\int_0^{T_F} c(t) dt = \frac{\hat{d}\sigma}{\lambda} \sum_{i=1}^N (1 - e^{\lambda(t_i - T_F)}) = \frac{\hat{d}\sigma}{\lambda} \left(N - \sum_{i=1}^N e^{\lambda(t_i - T_F)} \right) \quad (4.5)$$

and

$$\int_0^{T_F} u(t) dt = \sigma N \hat{d}. \quad (4.6)$$

As our main intention is keeping the concentration in a steady state, what we will do now is setting the results got for $c(t) \equiv c_d$ equal to the ones got for the general formula of $c(t)$. This is, $c_d T_F = \frac{\hat{d}\sigma}{\lambda} \left(N - \sum_{i=1}^N e^{\lambda(t_i - T_F)} \right)$ and $\lambda c_d T_F = \sigma N \hat{d}$.

As these two equations are not compatible, we will be using the first one to determine the doses \hat{d} depending on the other parameters. Therefore, we will consider

$$\hat{d} = \frac{c_d T_F \lambda}{\sigma \sum_{i=1}^N (1 - e^{\lambda(t_i - T_F)})} \quad (4.7)$$

as the dose administered with the aim of keeping $c(t)$ close to a steady state. Nonetheless, we have observed that there is not a big difference between the values of the integrals of $u(t)$ for the constant and the discrete cases in our experiments.

4.1.2 Temozolomide

Some parameters, as we have just said, can be deduced based on the drug and the type of tumor considered. In [10], the authors carry out experiments on mice. These mice had been implanted Lewis lung carcinoma cells in the proximal dorsal mid-line. For our computational experiments, we will be using Temozolomide (TMZ). This drug is usually administered as a treatment against brain tumors, although it can also be used against lung tumors.

For TMZ, $\lambda = 9.242 \text{ days}^{-1}$ (see [8]). Usually, Δ is taken as the half-life of the drug, $\Delta \approx \frac{\log 2}{\lambda}$ (see [19] and [6]), which corresponds to $\Delta = 0.075 \text{ days} = 1.8 \text{ hours}$. Additionally, its volume of distribution is $V_D = 0.4 \text{ L/kg}$ (see [15]). V_D can help us calculate σ . Supposing that our patient is a woman (therefore $\alpha = 1.6 \text{ m}^2$, see [18]) whose weight is $\beta = 60 \text{ kg}$, we get $\sigma = \frac{\alpha}{V_D \beta} = \frac{1.6}{0.4 \cdot 60} = \frac{1}{15} \approx 0.067 \text{ m}^2/\text{L}$.

We also know that a dose of 200 mg/m^2 appears to be maximum for a treatment. Therefore, considering the interpretation of k_2 that was given in the former chapter ($k_2 = \text{EC50}$) we can deduce that $0 < k_2 < \sigma \cdot 200 = \frac{200}{15} \approx 13.33 \text{ mg/L}$. We also consider $k_1 > 1$.

Furthermore, as the smallest commercialized capsules of TMZ weight 5 mg , we can consider that a 2 mg/m^2 treatment is not effective. As well, a 50 mg/m^2 treatment is used sometimes, so we think that it must be effective. Note that in Chapter 3 we mentioned that, in order to appreciate drug's influence on the tumor's evolution, it was necessary that $\alpha(t) = 1 - \frac{k_1 c(t)}{k_2 + c(t)} < 0$, which is equivalent to $c(t) > \frac{k_2}{k_1 - 1}$. From this, we deduce that

$$0.134 \approx 2\sigma < \frac{k_2}{k_1 - 1} < 50\sigma \approx 3.34. \quad (4.8)$$

We can give some values to k_1 and to k_2 that make the last inequalities true, and this choice will be very relevant, as we explain in the next section.

4.2 Cytotoxic treatment

We include in this section different figures showing the importance of the parameters' choice. First, we start by fixing the parameters as mentioned above:

- The parameters depending on the tumor were chosen according to [10]. Therefore, $\lambda_1 = 0.192 \text{ days}^{-1}$, $\lambda_2 = 0 \text{ days}^{-1}$, $b = 5.85 \text{ days}^{-1}$, and $d = 0.00873 \text{ days}^{-1}\text{mm}^{-2}$.
- Regarding the treatment and the times of administration, we consider a cytotoxic non-antiangiogenic ($e = 0$) treatment with TMZ. Because of this, we take $\Delta = 2$ hours (rounding the half-life value for simplicity), and we will suppose $T_F = 200$ days, from where we get $N = 2400$.
- Furthermore, supposing that the patient is a woman who weights 60kg, we consider $\sigma = 0.067 \text{ m}^2/\text{L}$ as we have just explained. Consequently, the values k_1, k_2 that we need to take must accomplish (4.8), and we choose them in order to make the fraction as small as possible.

Table 4.1 presents these parameters in a more visual way:

λ_1 day ⁻¹	λ_2 day ⁻¹	b day ⁻¹	d day ⁻¹ mm ⁻²	V_c mm ³	e day ⁻¹ kgmg ⁻¹	Δ hour	T_F day	σ m ² /L
0.192	0	5.85	0.00873	17347	0	2	200	0.067

Table 4.1: Parameters.

4.2.1 Choice of k_1 and k_2

It is clear that there are infinite pairs of numbers k_1, k_2 that make (4.8) true and give a similar value for the quotient $\frac{k_2}{k_1 - 1}$:

k_1	k_2	$\frac{k_2}{k_1 - 1}$
45	6	0.1364
21	3	0.1500
3.2	0.3	0.1364
1.7	0.1	0.1429

Table 4.2: Different possible values for k_1 and k_2 with a similar quotient $\frac{k_2}{k_1 - 1}$.

In order to decide which one of these possible pairs we are going to use, let us take into account that $k_2 = EC50$ and we will, thereby, consider it on the order of c_d . So, we will take in the rest of our experiments $k_1 = 1.7$, $k_2 = 0.1$ and $c_d = 0.4\text{mg}/\text{L}$, but we include in this subsection some examples showing the effect that a different choice would have on the results.

We will define an event as a final situation, where either the volume of the tumor decreases to almost 0 or it is near enough to the maximum volume, which would be considered as

a fatal situation for the patient. Making use of MATLAB, we will be able to determine the time at which an event takes place depending on the different parameters and initial points.

k_1	k_2	c_d	Event	Day of the event
1.7	0.1	0.4	$V \approx 0$	53.99
		1.5	$V \approx 0$	32.42
45	6	0.4	$V \approx 0$	10.43
		1.5	$V \approx 0$	2.51

Table 4.3: $(V_0, K_0) = (8000, 5000)$

We observe in Table 4.3 that, although for the initial point $(V_0, K_0) = (8000, 5000)$ both pairs lead to the same situation for the same concentrations, the times seem much more realistic when $k_1 = 1.7$ and $k_2 = 0.1$.

But we can find even more differences: depending on the pair (k_1, k_2) chosen, different events can take place for the same initial point and concentration.

k_1	k_2	c_d	Event	Day of the event
1.7	0.1	0.4	$V \approx 0$	120.56
		1.5	$V \approx 0$	76.78
45	6	0.4	$V \approx V_c$	0.12
		1.5	$V \approx V_c$	0.02

Table 4.4: $(V_0, K_0) = (16500, 2000)$

Table 4.4 shows how, for $(V_0, K_0) = (16500, 2000)$, different events take place depending on k_1 and k_2 , being again more realistic the times obtained for $k_1 = 1.7$ and $k_2 = 0.1$. Therefore, these two tables are a clear example of the importance of the parameters and why they should be checked by specialists.

4.2.2 Administration in N doses

As we have mentioned before, we are considering that TMZ is administered in discrete doses and, as we explained in the former chapter, the concentration is not going to be exactly c_d during all the treatment. Instead, it will present jump discontinuities at the times in which the doses are administered. We have calculated, using (4.7), the recommended value for each dose in order to keep concentration as close to $c_d = 0.4\text{mg/L}$ as possible. To obtain this value, we have taken $T_F = 200$, which, taking Δ as mentioned, leads us to $N = 2400$, and $d_i = \hat{d} = 4.6\text{mg/m}^2$, $i = 1 \dots N$. Note that this mode of administration corresponds to a metronomic-type therapy (see [8] and [13]). Figure 4.1

represents how would the concentration $c(t)$ evolve for these parameters during the first two days, and the blue line represents the constant value $c_d = 0.4\text{mg/L}$:

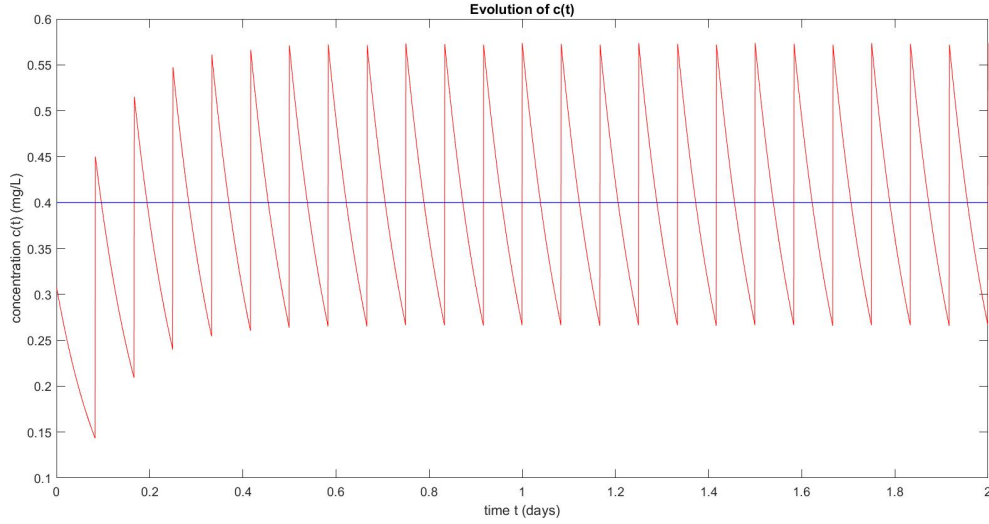


Figure 4.1: Evolution of the concentration during the first two days of treatment.

If we administer, instead, the same quantity of drug in each dose ($\hat{d} = 4.6\text{mg/m}^2$) but spacing the administration times differently, the concentration of drug in the body evolves in a very different way, and we show it for $t \in [0, 2]$ (it behaves similarly for $t \in [0, 200]$):

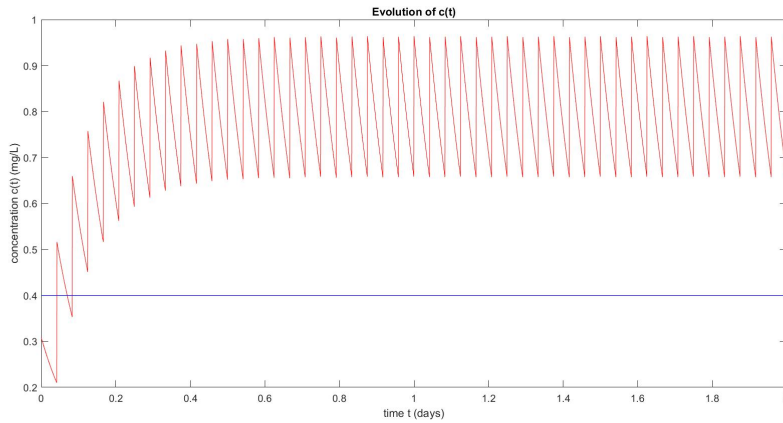


Figure 4.2: Evolution of $c(t)$ during the first two days if the drug is administered every hour

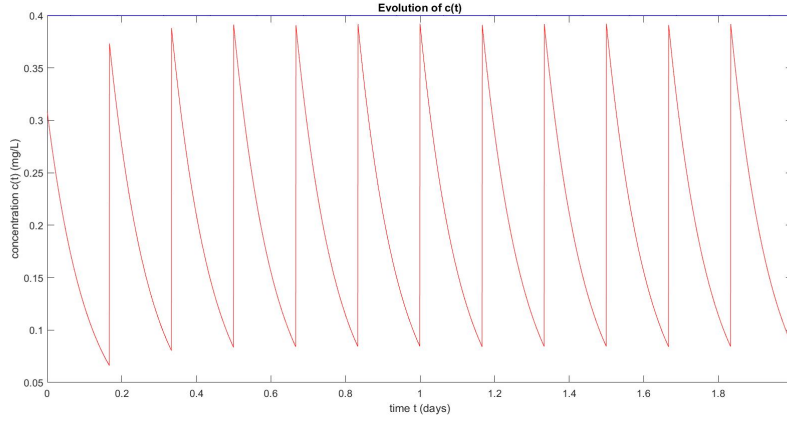


Figure 4.3: Evolution of $c(t)$ during the first 2 days if the drug is administered every 4 hours.

We observe that, if the doses are administered very frequently (less than 1.8 hours) then the concentration will remain too high. Instead, if they are given with many hours of difference, then the concentration of drug in the body may not reach the desired level. We have observed that perturbations of 10% on the administration times do not have great impact on the evolution of $c(t)$ nor on its effects.

AUC

When we take $\hat{d} = 4.6 \text{ mg/m}^2$ ($c_d = 0.4 \text{ mg/L}$), AUC in $[0, 200]$ is 80 for a constant administration, and for the discrete treatment too (if we consider N as the one given by administering the drug according to $\Delta = 1.8$ hours). Nonetheless, due to numerical approximations, we may observe slight differences between $\text{AUC}_{\text{constant}}$ and $\text{AUC}_{\text{discrete}}$, when considering other periods of time: this is, for example, what happens if we consider a final time \hat{T}_F such that $\hat{T}_F \neq \hat{N}\Delta$ for some $\hat{N} \in \mathbb{N}$ (note that, for our parameters, $200 = T_F = N\Delta$ with $N = 2400$ and $\Delta = 2/24$ days).

4.2.3 Initial points

We have already mentioned, in the previous chapters, how important the initial point is: depending on its location in the VK portrait, the behavior of the solution may vary (see Figure 2.3, for example). We consider different initial points to show the evolution of their volume and vasculature after applying a constant treatment, a treatment of N doses, and without treatment. We find it interesting to take the initial points in different regions of the VK portrait, focusing on points from the abnormal zone (those where the volume increases reaching the maximum volume: a fatal situation). Due to numerical reasons, we are considering $V(t) \approx V_c$ when $|V(t) - 0.995V_c| \leq 10^{-4}$.

Initial points in the abnormal zone

Note that, when no drug is administered, every initial point will lead to a fatal situation, as we explained in Chapter 2. Nevertheless, when a cytotoxic drug is given, this outcome depends on the initial point.

The regions in which $V(t)$ reaches V_c change depending on $c(t)$ for a fixed pair (k_1, k_2) . In Figure 4.4 we show the abnormal region obtained for a constant concentration $c_d = 0.4\text{mg/L}$, and $k_1 = 1.7, k_2 = 0.1$ (the grid becomes more precise when $V > 15000$ in order to get more accuracy).

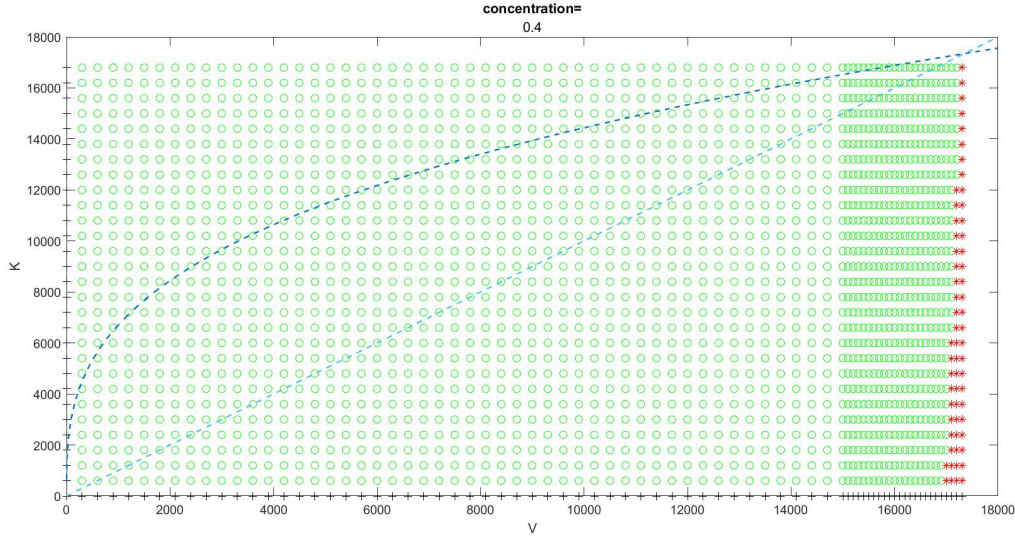
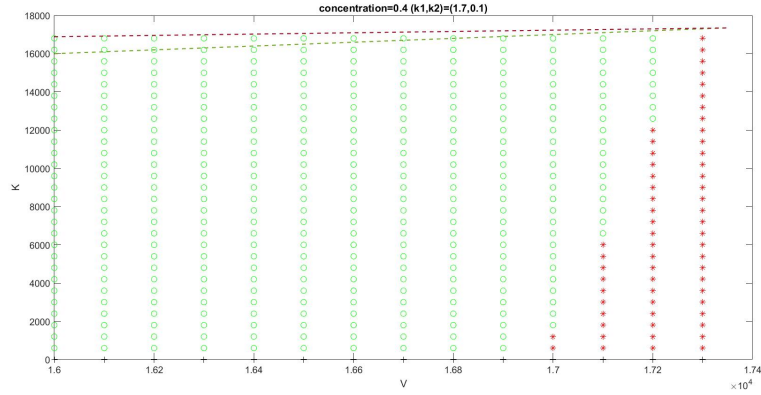
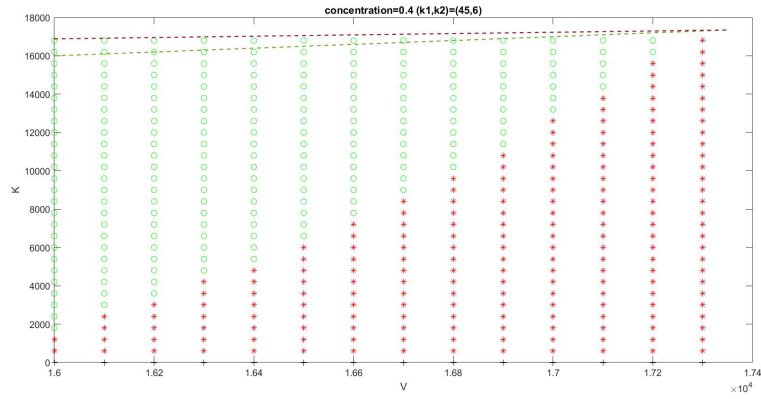
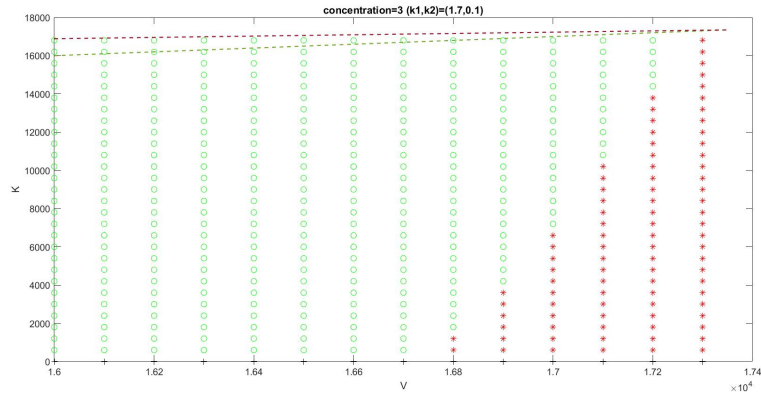


Figure 4.4: Abnormal region in red for a constant treatment of $c_d = 0.4\text{ mg/L}$ and $k_1 = 1.7, k_2 = 0.1$

This region may change when considering different concentrations, and when the treatment consists of N doses instead of a continuous infusion. In fact, we have observed that this region is highly related to $\frac{k_1 c(t)}{k_2 + c(t)}$:

- Zoomed in, Figure 4.4 becomes Figure 4.5 ($c_d = 0.4\text{ mg/L}$, $k_1 = 1.7, k_2 = 0.1$).
- For the same fixed concentration $c(t) \equiv c_d = 0.4\text{ mg/L}$, but for $k_1 = 45$ and $k_2 = 6$, we have Figure 4.6.
- For the same values $k_1 = 1.7$ and $k_2 = 0.1$, but for a different constant concentration $c_d = 3\text{ mg/L}$, the new abnormal zone is the one we present in Figure 4.7.

Figure 4.5: Zoom of the abnormal zone for a constant treatment of $c_d = 0.4$ mg/LFigure 4.6: Abnormal zone for different k_1 and k_2 ($k_1 = 45$, $k_2 = 6$)Figure 4.7: Abnormal zone for a different c_d ($c_d = 3$ mg/L).

Therefore, due to the variations in $c(t)$ given by the mode of administration, and the effects of the level of treatment on the abnormal region that we have shown in the previous figures, we can deduce that the abnormal zone is different when considering a treatment of N doses instead of a constant one. This means that, in some cases, when having a patient whose initial situation could be located in the abnormal zone for a certain mode of administration (this is, with a fatal outcome), we may observe that another administration way would lead to a successful final situation, or vice-versa. We will show an example of this case in the next subsection.

Our initial points

We are taking (V_0, K_0) in the set $\{(2000, 10000), (10000, 11200), (12000, 6000), (17000, 600), (17100, 600), (17100, 10000)\}$, being $(17000, 600)$ and $(17100, 600)$ in the abnormal zone for the constant treatment. We find it interesting to consider points in this zone because, as we have explained in the previous chapter, the behavior of the solutions seem counter intuitive when administering treatment.

Without administering any treatment, the VK portrait for these initial points looks as follows:

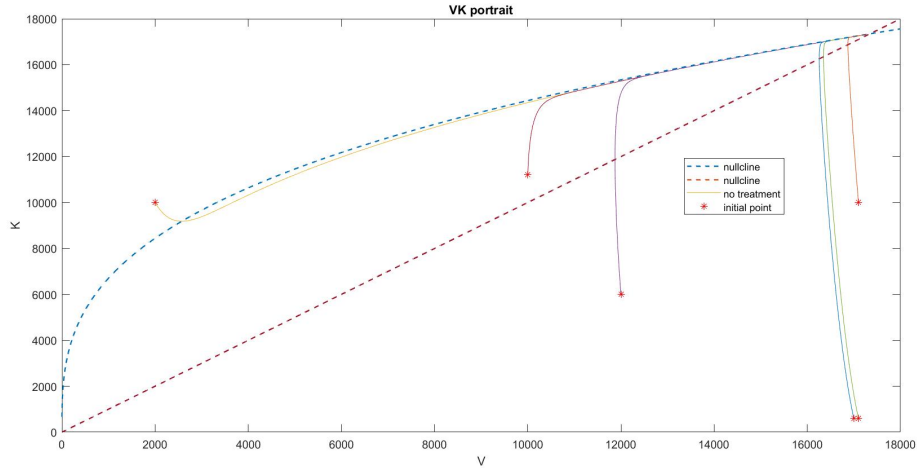


Figure 4.8: VK portrait without administering any treatment

We can easily observe that, according to what we explained in previous chapters, for the initial points under the red nullcline (the diagonal), the volume naturally decreases until it reaches other zones, where it starts growing tending to V_c , which corresponds to the point where the two nullclines intersect. The times for these events are presented in Table 4.5 in the next subsection.

4.2.4 Comparing administration ways

We can either suppose that the cytotoxic treatment is administered in a constant way (what might not be feasible in reality) or in a discrete mode, with N doses. We present in Table 4.5 a comparison of the events that take place for both different administration ways for the cytotoxic treatment and the times it takes to these events to take place. We also include a column presenting the effect of not administering any treatment.

(V_0, K_0)	No treatment		Continuous treatment		Discrete treatment		Best treatment
	Event	Time of the event (days)	Event	Time of the event (days)	Event	Time of the event (days)	
(2000, 10000)	$V \approx V_c$	48.02	$V \approx 0$	31.42	$V \approx 0$	31.85	Continuous
(10000, 11200)	$V \approx V_c$	37.32	$V \approx 0$	61.06	$V \approx 0$	61.46	Continuous
(12000, 6000)	$V \approx V_c$	34.62	$V \approx 0$	70.24	$V \approx 0$	70.34	Continuous
(17000, 600)	$V \approx V_c$	20.95	$V \approx V_c$	0.27	$V \approx 0$	152.98	Discrete
(17100, 600)	$V \approx V_c$	20.25	$V \approx V_c$	0.09	$V \approx V_c$	0.26	No treatment
(17100, 10000)	$V \approx V_c$	14.22	$V \approx 0$	150.61	$V \approx 0$	147.84	Discrete

Table 4.5

The next two figures show the VK portraits for the points of table 4.5 and the two different administration modes. Figure 4.9 corresponds to the constant treatment, where the patient would die in two of the six situations presented, whereas Figure 4.10 corresponds to the discrete one, where the fatal situation takes place in only one of the cases.

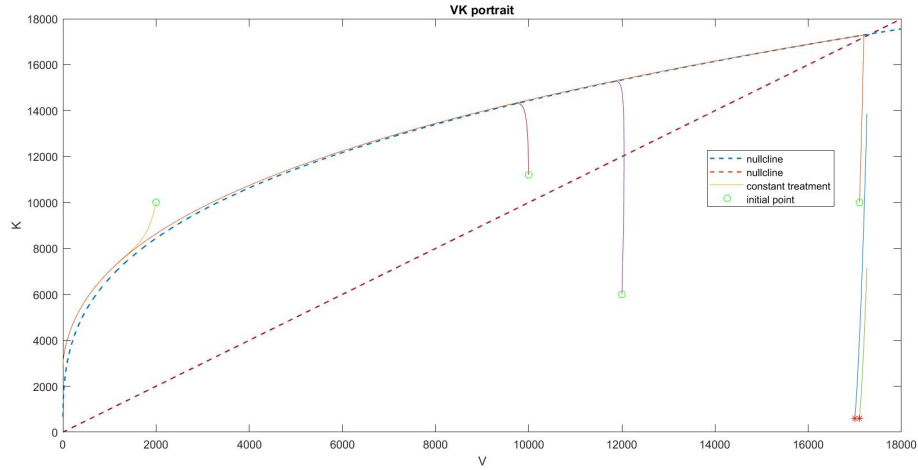


Figure 4.9: VK portrait for the constant treatment.

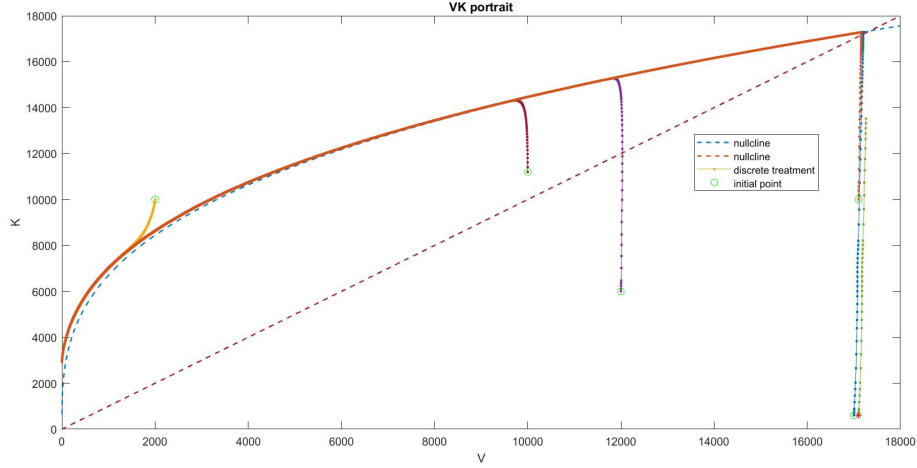


Figure 4.10: VK portrait for the discrete treatment.

Note that, now, when administering a cytotoxic treatment, the solutions tend to move to the right instead of leftwards when being under the diagonal. We will take this fact into account in the next section, that corresponds to mixing treatments.

By observing Table 4.5 and Figures 4.9 and 4.10, we can deduce several conclusions. We find that, as we have commented in the former section, the abnormal zone may vary depending on the mode of administration: for an initial point which, with a constant treatment developed into a fatal situation, such as $(V_0, K_0) = (17000, 600)$, a discrete treatment would lead to $V \approx 0$, being therefore $(V_0, K_0) = (17000, 600)$ in the abnormal zone for the constant treatment but not for the discrete one.

Another conclusion that can be deduced from the results presented in this table is that, even having the same initial volume V_0 , two points with different initial vasculature can lead to different events when given the same type of treatment. This is the case of $(V_0, K_0) = (17100, 600)$, which is in the abnormal zone for both the constant and the discrete treatments, and $(V_0, K_0) = (17100, 10000)$, which is in the other zone despite having the same initial volume.

The next figures show the evolution of the tumor volume depending on the administration mode for these 3 initial points, as well as for $(V_0, K_0) = (2000, 10000)$, which would be in the normal zone in all the cases:

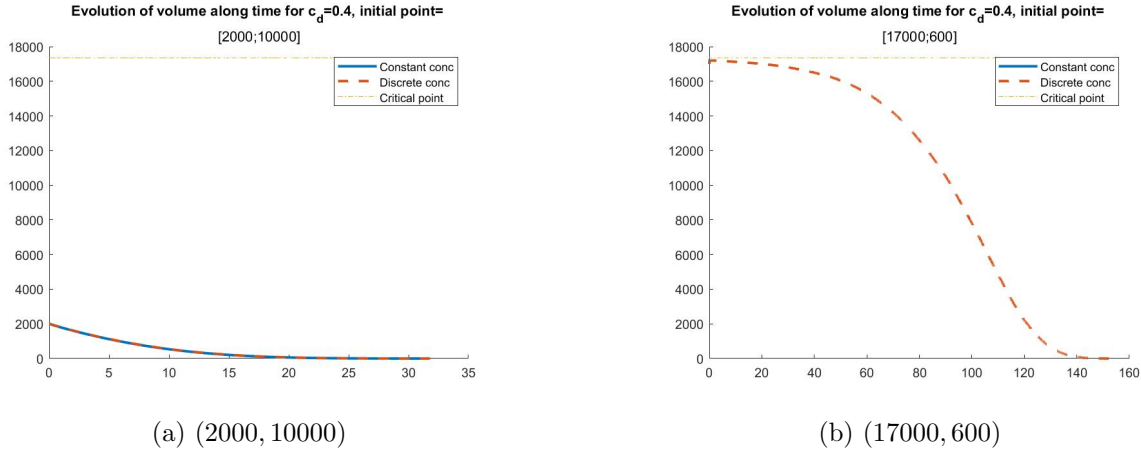


Figure 4.11: Evolution of volume along time for different initial points and modes of administration

It might be difficult to see, in Figure 4.11b, the blue continuous line, corresponding to a constant administration. This is because the time it takes to the tumor volume to be very close to V_c is very short compared to the time it takes to the volume to be almost 0 when administering the drug discretely.

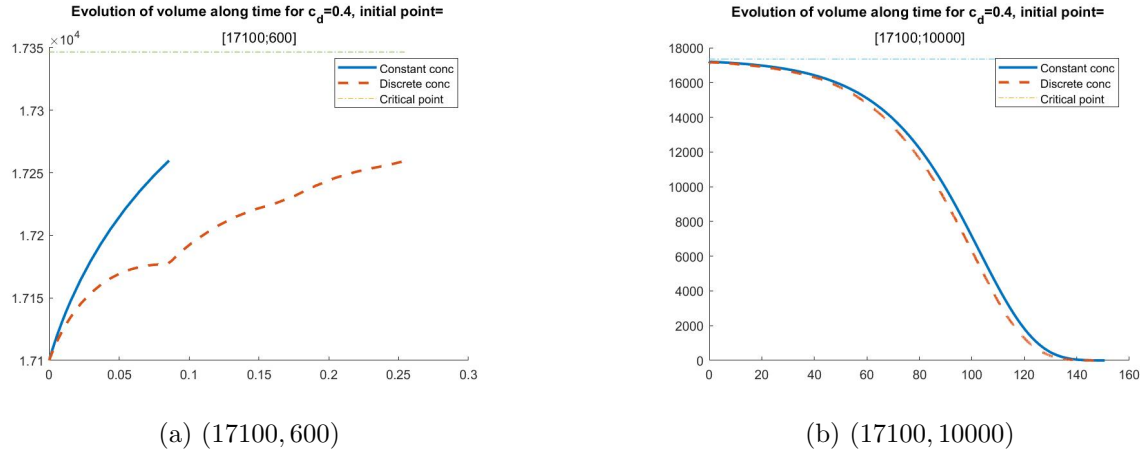


Figure 4.12: Evolution of volume along time with different modes of administration for initial points with the same initial volume but different vasculatures

This last figure shows us the relevance of the initial vasculature. Note that the evolution of volume has been studied until $V \approx 0.995V_c$, and this is why in Figure 4.12a the curves do not reach the line corresponding to the critical volume, although they would if we let the program calculate it.

4.3 Combining different treatments

We have already introduced, succinctly, what this section is based on: we have observed that, depending on whether we administer a cytotoxic treatment or not, the solutions behave differently. For instance, for points located in the normal zone, a cytotoxic treatment would lead to the healing of the patient. But not only this, we have also seen that administering treatment would fasten the fatal situation in some occasions (this was the case of some initial points that were in the abnormal zone for the cytotoxic treatment, as we have shown in Table 4.5). Therefore, one decision could be taken in order to improve the consequences of applying a cytotoxic treatment: as the abnormal zone is always located under the diagonal (where we observed that the solutions move rightwards when administering a cytotoxic drug), and knowing that, in this zone and without treatment, the volume would naturally decrease (although after some time it would reach other zones and increase again if no treatment was applied), what we can do is awaiting, without administering any drug, until the volume and the vasculature of the tumor reach the normal zone, in which we know it is always safe to inject the cytotoxic drug.

In Figure 4.13, we can observe the effects of applying this technique. The moment we have chosen to start applying treatment is when our MATLAB program detects that the volume of the tumor is starting to increase. Note that this technique is only applied, in this example, to the points where applying directly a cytotoxic treatment led to a fatal situation, because for the other ones we know it is safe to apply it since the first moment. This point is, for the administration in N doses, $(V_0, K_0) = (17100, 600)$ and now the patient would heal. Compare this figure to Figure 4.10 to appreciate easier these effects.

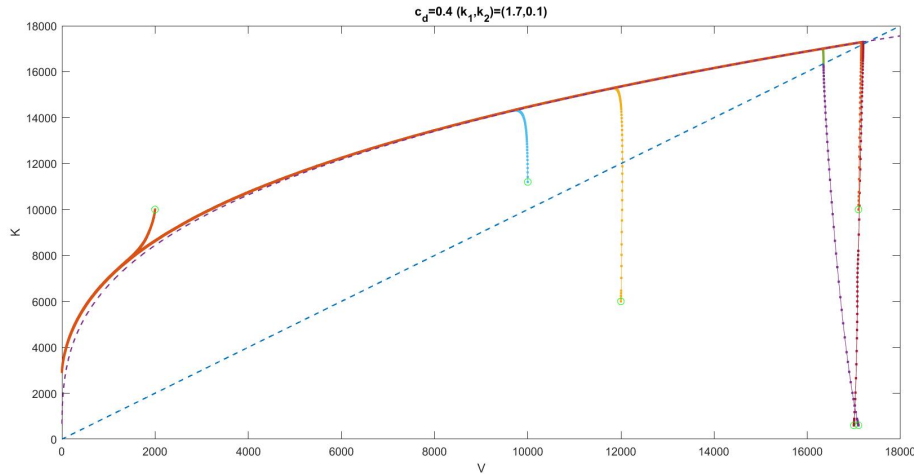


Figure 4.13: VK portrait after waiting some time before introducing treatment.

Something similar is what we are going to study along this section, although, basing

on the ideas of [11] we will combine an antiangiogenic non-cytotoxic treatment with a cytotoxic non-antiangiogenic one. We expect these studies to be relevant too because, as proved in section 2.2 of [13], if $b > \lambda_2 + ec_d$ then an antiangiogenic treatment diminishes the maximum volume reachable by the tumor, which implies that the solution will be able to “escape” the abnormal zone, as it did when we did not apply any treatment. Look at Figure 4.14, where only an antiangiogenic drug is administered, to see this (note that the critical point, the one towards which the solutions tend, has now a lower volume, as explained in [13]). We take $e = 2$ according to [3], being now the critical volume $\hat{V}_c = 13913$, according to Chapter 3 .

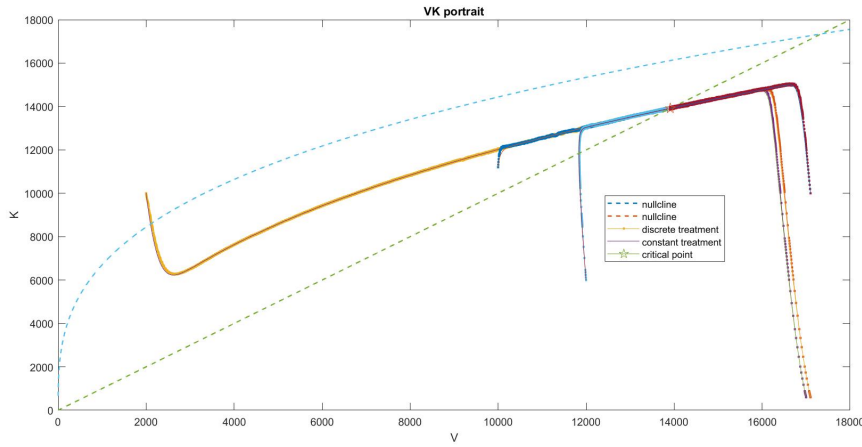


Figure 4.14: VK portrait with $k_1 = 0$ and $e = 2$

4.3.1 Combining treatments: experiments

Once introduced our motivation for doing these experiments, we include here some of the results we have obtained, which we find are the best to represent the different situations that can take place. We will, therefore, present the results for 3 normal initial points, and for an abnormal one. The points that we will be taking are the following:

- $(V_0, K_0) = (2000, 10000)$, whose behavior when administering a cytotoxic treatment, because of it being over the diagonal of the VK portrait, will be the expected: the volume will decrease as time goes by (see Figure 4.11a).
- $(V_0, K_0) = (12000, 6000)$, which is under the diagonal. At this point, when administering a cytotoxic drug, the volume starts to increase, but then, once the solution gets to the diagonal, it starts decreasing as it did for the former point, being therefore in the normal zone.
- $(V_0, K_0) = (17100, 10000)$, that is in the normal zone and under the diagonal. For this initial point the solution behaves as for $(V_0, K_0) = (12000, 6000)$.

- $(V_0, K_0) = (17100, 600)$, which is also under the diagonal. For this initial point, when administering a cytotoxic drug, the volume will reach the fatal volume (see Figure 4.12a), implying the death, which locates it in the abnormal zone.

We will apply, in a discrete way and considering the recommended doses according to what we have explained in the previous sections, pretending to maintain $c(t)$ close to $c_d = 0.4\text{mg/L}$, different treatment combinations in order to find the most suitable one.

Cytotoxic treatment

When we do not combine treatments and we only apply a cytotoxic treatment, the VK portrait and the results obtained for these initial points are presented in the former section, in Table 4.5.

Antiangiogenic treatment

If, instead, we only apply an antiangiogenic treatment with $e = 2$, the results would be the ones presented in Figure 4.14 with the dotted lines. In none of the cases would the volume of the tumor reach the fatal point, but neither would it be nullified.

Combination: First antiangiogenic, then cytotoxic

We will distinguish 2 cases: when it is necessary to combine treatments, because the patient would die if only a cytotoxic drug is administered, and when it is not.

For the first case, we will start by applying an antiangiogenic drug taking $k_1 = 0$ and $e = 2$, but considering the same parameters as before for the drug and the tumor. Once the volume is close enough to the volume of the new critical point (\hat{V}_c) , we will change the treatment to a cytotoxic non-angiogenic one. We are only applying this combination to the abnormal initial point. For the rest of the points, we will keep the cytotoxic treatment. The VK portrait now looks as follows:

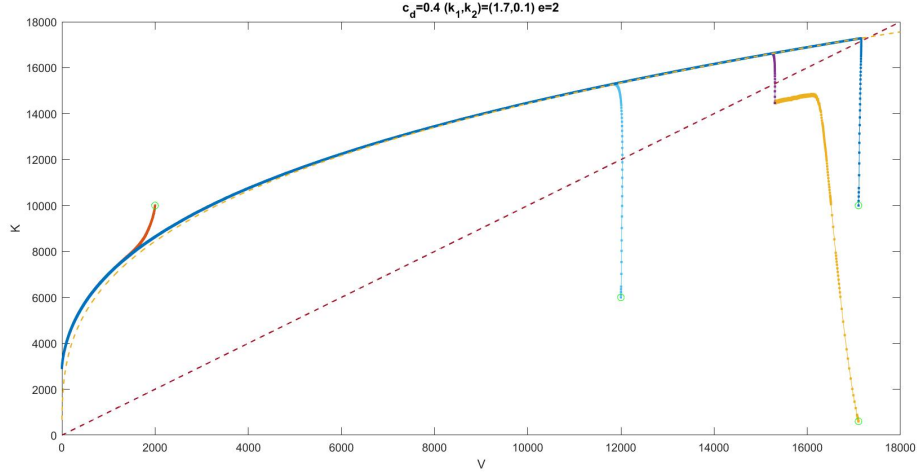
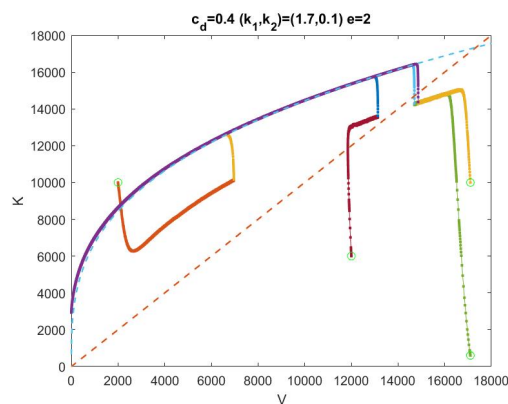


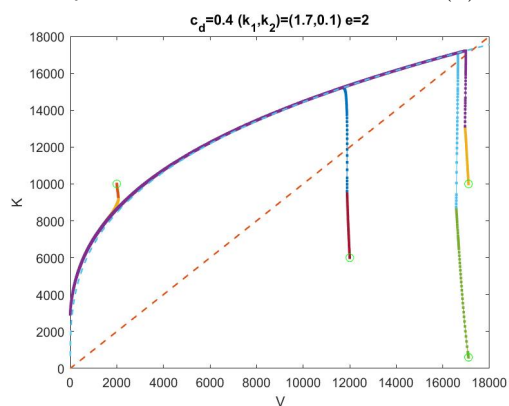
Figure 4.15: VK portrait when an antiangiogenic treatment is administered during the first 5 days in the case where applying directly a cytotoxic treatment would be fatal.

As it can be seen in Figure 4.15, applying an antiangiogenic treatment before the cytotoxic one is only needed for the initial point $(V_0, K_0) = (17100, 600)$ and a good moment to administrate the antiangiogenic one is, approximately, on day 5, although it could be given sooner, as the solution escapes the abnormal zone much earlier. We will show this in the next figures, where we provide the VK portraits obtained for different change-of-treatment times. Note that we will now apply the treatment combination to all the initial points, and not only to the abnormal one, that we are doing our experiments considering that the antiangiogenic drug has the same parameters as the cytotoxic drug, and that we are assuming that the desired constant concentration is the same for both treatments.

If we apply the second treatment after 30 days of administering the antiangiogenic drug, we observe in the VK portrait given in Figure 4.16a that, even if the patient would heal in the 4 situations and the healing would be accelerated almost 35 days for $(V_0, K_0) = (17100, 10000)$ (see Figure 4.17a), the first treatment worsens heavily the situation of the first two cases, stabilizing temporary the tumor size around 13913. Therefore, we have tried with a different change-of-treatment time, being Figures 4.16b and 4.17b the corresponding to 10 days of antiangiogenic treatment. We observe that, in this case, the situation for the two first initial points does not worsen as much as it did in the former case, and for $(V_0, K_0) = (17100, 10000)$ the healing takes place on day 99 instead of 147 (see Table 4.5), which makes us think of reducing even more the period of administration of the antiangiogenic drug. In fact, if we administered it during just 3 hours, the final results would be quite satisfactory for the first two cases (see 4.16c and 4.17c), although the healing of $(V_0, K_0) = (17100, 10000)$ would only be accelerated around 15 days.



(b) Change time = 10 days



(c) Change time = 3 hours

Figure 4.16: VK portraits. First antiangiogenic treatment, then cytotoxic.

These VK portraits correspond to the following figures, which represent the evolution of the volume against time:

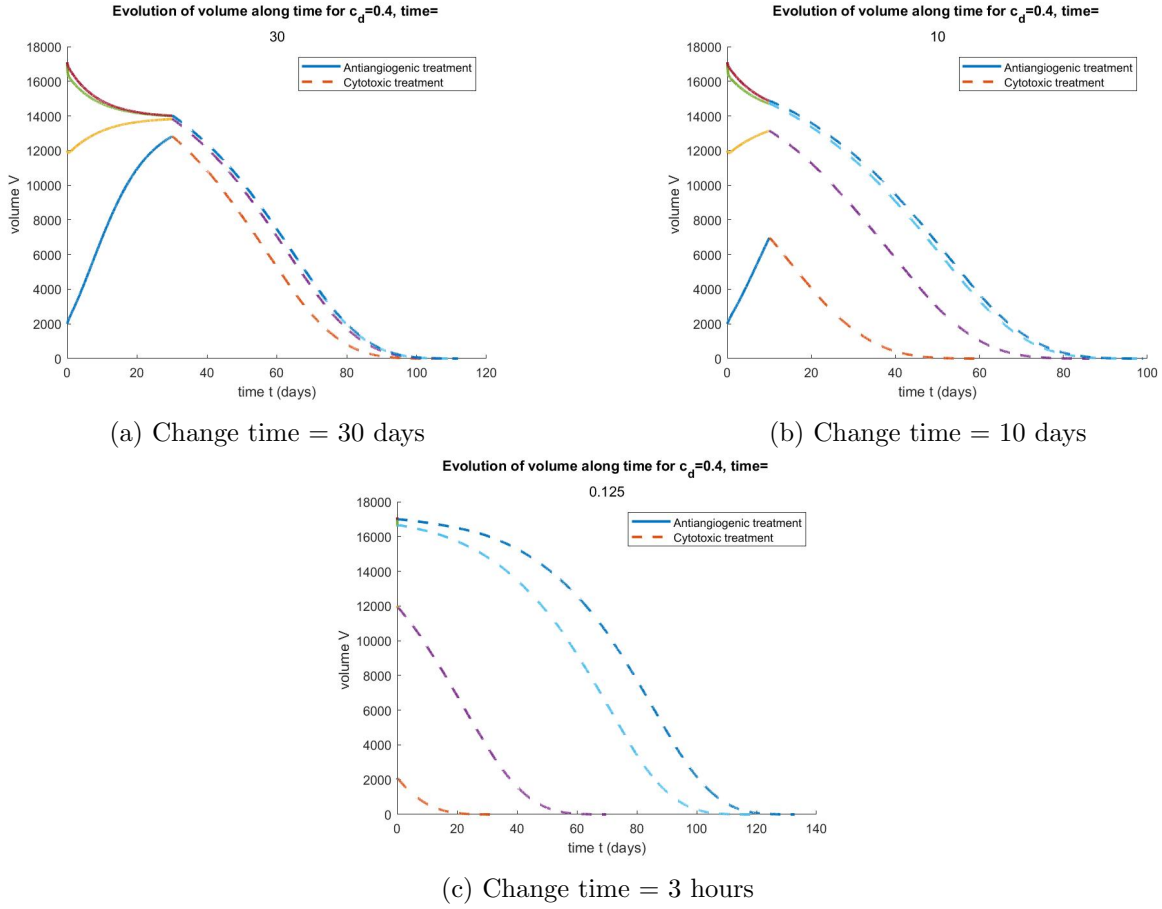


Figure 4.17: Evolution of tumor volume applying first an antiangiogenic treatment and then switching to a cytotoxic one.

We observe that even a very short period (according to the parameters chosen, this period may vary) of antiangiogenic treatment can have successful results, but the fact that not applying any treatment at the beginning could also have a beneficial impact (remember Figure 4.13) may cast doubts on the necessity of applying this kind of treatment. Nonetheless, we have noticed that the appliance of this treatment (against to not applying any treatment) could accelerate the healing of the patient, and we present a comparison of the healing times in Table 4.6. We can see in it that, the longer the period before administering the cytotoxic drug is, the bigger the difference between both options becomes. Note that when no treatment is administered during 30 days, a patient whose initial conditions were $(V_0, K_0) = (17100, 600)$ or $(V_0, K_0) = (17100, 10000)$ would be dead, being it too late to introduce the cytotoxic treatment.

Initial point	No treatment			Antiangiogenic treatment		
	30 days	10 days	3 hours	30 days	10 days	3 hours
(2000, 10000)	143.36	68.68	32.39	104.44	60.29	32.36
(12000, 6000)	181.01	105.22	69.89	110.54	86.21	69.76
(17100, 600)	Too late	145.81	118.66	111.78	97.72	118.08
(17100, 10000)	Too late	161.89	133.62	111.84	98.97	132.70

Table 4.6: Healing times, in days, when no treatment or an antiangiogenic treatment is administered at the beginning.

We can also observe that, clearly, this combination would be successful for the initial points located in the abnormal zone. Regarding the ones in the normal zone, we can conclude, comparing the healing times of Tables 4.5 and 4.6, that if their initial volume is smaller than the volume of the critical point for the antiangiogenic treatment (which we calculated, in previous chapters, as $\hat{V}_c = \left(\frac{b - ec_d - \lambda_2}{d} \right)^{\frac{3}{2}}$, and corresponds to 13913 mm^3 for our parameters) then this combination would not be very useful. Nonetheless, it could imply a substantial acceleration of the healing times when the initial volume is bigger than the critical one. These healing times will depend on the change-of-treatment times, which should be adjusted considering other external factors such as side effects.

Combination: First cytotoxic, then antiangiogenic

For this case we have two different options: whether to extend the first period, corresponding to the cytotoxic treatment, the time enough to make the tumor disappear for the points in the normal zone (this would be fatal in the abnormal zone) or to shorten this period, which would make the tumor size stabilize, but not nullify (if a fatal situation does not occur before changing the treatment). The next figures may help to understand what we mean:

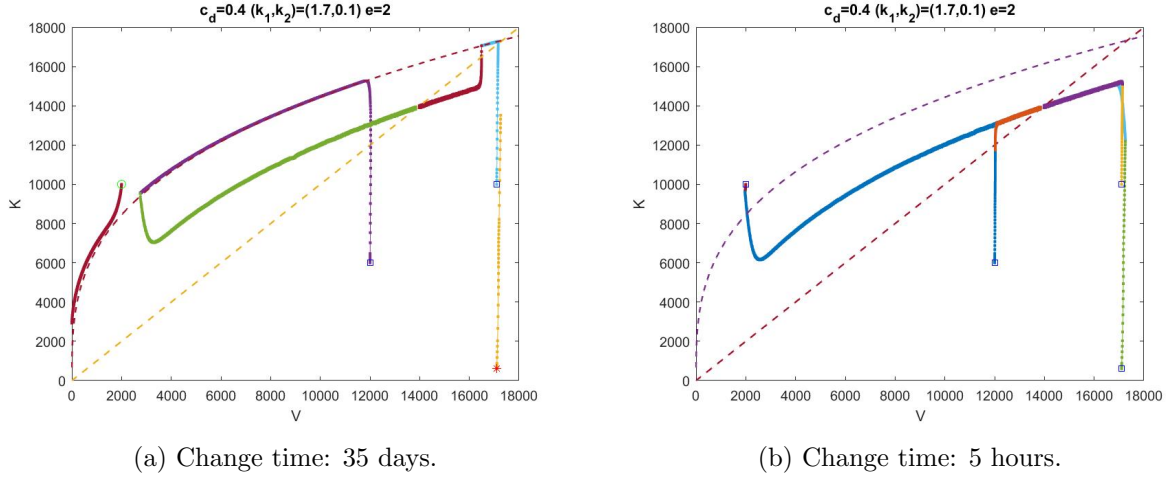


Figure 4.18: VK portraits applying first a cytotoxic treatment and then switching to an antiangiogenic one.

When applying a cytotoxic treatment to a tumor whose initial conditions were $(V_0, K_0) = (2000, 10000)$, we observed that it took approximately 32 days to the volume to be almost nullified (see Table 4.5). In the case of a tumor with initial conditions equal to $(V_0, K_0) = (12000, 6000)$ (resp. $(V_0, K_0) = (17100, 10000)$) it took a bit longer: around 70 (resp. 148) days. And, when the tumor volume and vasculature were $(V_0, K_0) = (17100, 6000)$, we found out that a cytotoxic treatment would be lethal in less than a day. Therefore, Figure 4.18a represents perfectly the two options mentioned above: for the first point, choosing a first period long enough ($35 > 32$) would be as beneficial as just applying a cytotoxic treatment, as the patient would heal before applying the antiangiogenic one and this last would not be necessary. Nevertheless, taking this period would not be as successful as for this point for the rest of the points: we can observe that, when considering $(V_0, K_0) = (12000, 6000)$ and $(V_0, K_0) = (17100, 10000)$, as neither the best situation nor the fatal one take place before changing the treatment, the volume stabilizes around 13913, as it did when only administering an antiangiogenic drug. The worst situation is the one of the last point, because the patient would die before being able to change treatments. For our parameters and our initial points, changing the treatment after at most 5 hours would avoid the fatal situation, but none of the cases would see its volume nullify (see Figure 4.18b).

What is interesting about this combination is noticing that, even when it does not cure the patient, it can decelerate its tumor size stabilization: it would take only 32 days to the tumor corresponding to the second point to have its volume almost unvarying if we applied the cytotoxic drug during the first 5 hours whereas it takes almost 90 days when administering it during 35 days (vs 37.50 if we did not apply any cytotoxic drug before). This can be seen in Figure 4.19, which corresponds to the VK portraits of Figure 4.18.

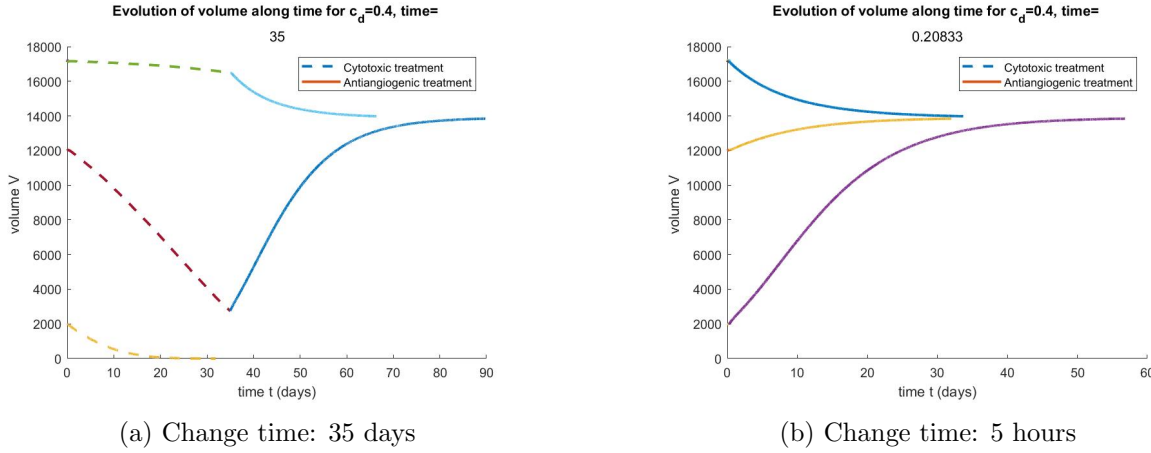


Figure 4.19: Evolution of volume applying first a cytotoxic treatment and then switching to an antiangiogenic one.

Note that in Figure 4.19a we cannot appreciate the evolution of the tumor volume corresponding to the initial point $(V_0, K_0) = (17100, 600)$ because it reaches the fatal volume very soon (the higher line corresponds to $(V_0, K_0) = (17100, 10000)$). Something similar occurs in Figure 4.19b, where the period of administration of the cytotoxic treatment is very short compared to the antiangiogenic one, not being noticeable in our figure. In Figure 4.19b the lines for the points with initial volume 17100 are almost coincident, and they give the impression of being just one. Neither can we see, in Figure 4.19a, the line corresponding to the antiangiogenic treatment for $(V_0, K_0) = (2000, 10000)$ because the patient would heal before the change time, so the second treatment would not be applied.

4.4 MATLAB programs

For our study, we have implemented several MATLAB programs. The most relevant ones have been the programs for the VK portraits, the ones for the evolution of tumor volume and vasculature against time and the ones for concentration.

The programs for the VK portraits, as well as the volume-vasculature versus time ones, are based on the MATLAB function *ode45*. As inputs, we have implemented different functions, depending on the model used, the kind of treatment and the administration way. We have also implemented the *events* function, which is necessary to get as outputs the times of the events (in our work, they correspond to the moments in which the volume was small enough or very close to the critical volume or the fatal volume) and the solutions at that times. These outputs are the ones that appear in many of our tables, and they have been useful to determine the change-of-treatment times, being the initial conditions for the new treatments. The *events* function has one more output, which we have used to know the outcome of applying treatment in order to determine if an initial

point corresponded to the abnormal zone or not.

To study the concentration evolution we have implemented a function according to (3.4), which we have represented using different plotting functions of MATLAB. We have also used this function to see the effect of a discrete concentration on the tumor evolution.

Combining these programs, their outputs and other MATLAB functions such as *tiledlay-out* we have been able to obtain the figures, tables and results presented in our report. The version of MATLAB that we have been using is MATLAB R2021a.

Chapter 5

Conclusions

In this work we have studied the evolution of cancer tumors in both a non-perturbed situation and a perturbed one, when a drug is administered. In order to do so, we required different parameters and we have distinguished the different cases that can take place according to them. It is noteworthy that we have done our study considering a dynamic vasculature because, due to angiogenesis, it varies along time. But not only does the vasculature change according to time: the concentration of the drug administered is time-dependant too, according to pharmacokinetics. Therefore, our study considers both the case in which this concentration remains constant and the case in which it does not.

In our computational experiments, we have firstly considered a cytotoxic treatment with TMZ, administered in different doses. We have determined the administration times that make the concentration of the drug in the body as constant as possible, and compared the resultant discrete treatment to a continuous administration.

Moreover, we have verified (both in our theoretical study and in our computational experiments) a fact that had already been noticed in clinical studies: depending on the initial conditions, administering a cytotoxic drug can worsen the situation, stimulating tumor growth. Although it remains a mystery, new theories blame it on cell “debris”:

- [5]: “The presence of dead material within a tumor could affect tumor dynamics in terms of volume loss (...), as the tumor volume may even increase at the initial stages of treatment due to the coexistence of (...) and of an increasing dead material not yet adequately drained off”.
- [9]: “Therapy can be a double-edged sword”; “Despite the effectiveness of chemotherapy (...), chemotherapy may stimulate tumor growth”; “Killing cells generates cell “debris” which can promote tumor progression”.
- [7]: “Chemotherapy (...) can result in the emergence of drug-resistant cells which ultimately lead to tumor regrowth and therapy failure”.

This is why we have identified two separated zones when administering treatment: a normal one, for the initial conditions for which the patient heals, and an abnormal one, which corresponds to the points in which this counter intuitive situation takes place, leading to a fatal outcome. We have carried out our computational experiments considering both situations, referring to which we have obtained two important conclusions:

- We have seen that the abnormal zone varies depending on the patient and the tumor considered, as well as on the drug and the way it is administered (which could be seen comparing Figures 4.9 and 4.10). The choice of parameters k_1 and k_2 has a noteworthy impact on the abnormal section too, as we showed in Figures 4.5, 4.6 and 4.7, and they should be determined by a specialist in order to make the results more accurate.
- At first, it seems logic to expect that, whether a patient heals or not when administering a cytotoxic drug depends on how proximate its initial tumor volume is from the fatal volume. Nevertheless, we have observed that not only the initial tumor volume will affect in its evolution, but also its initial vasculature. This is why the boundary between the normal and the abnormal zones in the VK portraits does not correspond to a vertical line. We have shown, as an example, in Figure 4.12 the volume evolution of two different tumors which had the same initial volume, but different initial vasculature, leading to two different final situations. This means that we can not determine if a tumor will, or not, behave as expected when administering the drug by only looking at its initial volume without taking into account its vasculature.

Aiming to face the problems posed by the administration of a cytotoxic drug, combined therapies (with antiangiogenic drugs) could be a reliable alternative. This is what we have shown in the last section of Chapter 4, where we have presented two different combinations. The conclusions for the second combination are mentioned in this chapter. The ones for the first combination are also explained in this fourth chapter, but we consider they are noteworthy: it is true that, according to our parameters, for some points in the normal zone the healing times would not differ significantly from the ones with just a cytotoxic treatment. Nevertheless, we have found out that for the initial points in the abnormal zone this combination would result in a fortunate outcome. Moreover, we have seen that, even for initial points where the cytotoxic treatment was successful by itself, this combination could accelerate notably the healing times when the initial volume is above a certain level, which also depends on the parameters.

It is clear that the transition from bench to bedside is not simple, and that many external factors must be taken into account in order to cure or shrink a tumor, existing innumerable strategies whose consequences may not be clearly determined. Nonetheless, we hope that this study may be useful to reduce the wide range of options to be considered, diminishing therefore the elevated costs they entail.

Bibliography

- [1] L. Aguilera. *Conceptos básicos de Farmacocinética Farmacodinámica en TIVA*. URL: http://www.sld.cu/galerias/pdf/sitios/anestesiologia/tiva_conceptos_basicos.pdf.
- [2] S. Benzekry et al. “Classical Mathematical Models for Description and Prediction of Experimental Tumor Growth”. In: *PLoS Computational Biology* 10.8 (Aug. 2014). DOI: 10.1371/journal.pcbi.1003800. URL: <https://dx.plos.org/10.1371/journal.pcbi.1003800>.
- [3] M. Bodzioch, P. Bajger, and U. Foryś. “Angiogenesis and chemotherapy resistance: optimizing chemotherapy scheduling using mathematical modeling”. In: *Journal of Cancer Research and Clinical Oncology* 147 (May 2021), pp. 2281–2299. DOI: 10.1007/s00432-021-03657-9. URL: <https://link.springer.com/10.1007/s00432-021-03657-9>.
- [4] P. Carmeliet and R. K. Jain. “Angiogenesis in cancer and other diseases”. In: *Nature* 407 (Sept. 2000), pp. 249–257. DOI: 10.1038/35025220. URL: <https://www.nature.com/articles/35025220>.
- [5] P. Castorina et al. “Tumor Volume Regression during and after Radiochemotherapy: A Macroscopic Description”. In: *Journal of Personalized Medicine* 12.4 (Mar. 2022), p. 530. DOI: 10.3390/jpm12040530. URL: <https://www.mdpi.com/2075-4426/12/4/530>.
- [6] *Curso “Saber de farma”*. URL: <https://edruida.com/cursos/saber-de-farma/>.
- [7] C. D’Alterio et al. “Paradoxical effects of chemotherapy on tumor relapse and metastasis promotion”. In: *Seminars in Cancer Biology* 60 (Feb. 2020), pp. 351–361. DOI: 10.1016/j.semcancer.2019.08.019. URL: <https://linkinghub.elsevier.com/retrieve/pii/S1044579X19301749>.
- [8] L. A. Fernández, C. Pola, and J. Sáinz-Pardo. “A mathematical justification for metronomic chemotherapy in oncology”. In: *Mathematical Modelling of Natural Phenomena* 17 (2022). Article: 12. DOI: 10.1051/mmnp/2022010. URL: <https://www.mmnp-journal.org/10.1051/mmnp/2022010>.
- [9] V. M. Haak, S. Huang, and D. Panigrahy. “Debris-stimulated tumor growth: a Pandora’s box?” In: *Cancer and Metastasis Reviews* 40 (Sept. 2021), pp. 791–801. DOI: 10.1007/s10555-021-09998-8. URL: <https://link.springer.com/10.1007/s10555-021-09998-8>.

- [10] P. Hahnfeldt et al. “Tumor development under angiogenic signaling: a dynamical theory of tumor growth, treatment response, and postvascular dormancy”. In: *Cancer Research* 59 (Oct. 1999), pp. 4770–4775.
- [11] R. K. Jain. “Normalizing tumor vasculature with anti-angiogenic therapy: A new paradigm for combination therapy”. In: *Nature Medicine* 7 (Sept. 2001), pp. 987–989. DOI: 10.1038/nm0901-987. URL: <https://www.nature.com/articles/nm0901-987>.
- [12] L. Norton and R. Simon. “Tumor size, sensitivity to therapy, and design of treatment schedules.” In: *Cancer treatment reports* 6 (Oct. 1977), pp. 1307–1317. URL: <https://pubmed.ncbi.nlm.nih.gov/589597/>.
- [13] M. Peña. “Analysis and optimization of a mathematical model for the growth and treatment of cancerous tumors including angiogenesis”. L.A. Fernández (dir.). Trabajo fin de grado, Grado en Matemáticas de la Universidad de Cantabria. PhD thesis. Universidad de Cantabria, 2022.
- [14] International Agency for Research of Cancer. *900 world fact sheets*. URL: <https://gco.iarc.fr/today/data/factsheets/populations/900-world-fact-sheets.pdf>.
- [15] *Temozolomide: Uses, Interactions, Mechanism of Action*. URL: <https://go.drugbank.com/drugs/DB00853>.
- [16] T. N. Tozer and M. Rowland. *Introduction to Pharmacokinetics and Pharmacodynamics: The Quantitative Basis of Drug Therapy*. Lippincott Williams & Wilkins, 2006.
- [17] *What is Cancer?* 2007. URL: <https://www.cancer.gov/about-cancer/understanding/what-is-cancer>.
- [18] *Wikipedia: Área de superficie corporal*. URL: https://es.wikipedia.org/wiki/%C3%81rea_de_superficie_corporal.
- [19] *Wikipedia: Biological half-life*. May 2023. URL: https://en.wikipedia.org/w/index.php?title=Biological_half-life&oldid=1157293041.
- [20] *Wikipedia: Volume of Distribution*. 2022. URL: https://en.wikipedia.org/w/index.php?title=Volume_of_distribution&oldid=1120386504.
- [21] C. P. Winsor. “The Gompertz Curve as a Growth Curve”. In: *Proceedings of the National Academy of Sciences* 18 (June 1932), pp. 1–8. DOI: 10.1073/pnas.18.1.1. URL: <https://pnas.org/doi/full/10.1073/pnas.18.1.1>.